別紙４

研究成果の刊行に関する一覧表

書籍

著者氏名	論文タイトル名	書籍全体の編集者名	書　籍　名	出版社名	出版地	出版年	ページ

雑誌

発表者氏名	論文タイトル名	発表誌名	巻号	ページ	出版年
S Murata, Y Koga, Y Moriya, T Akasu, S Fujita, S Yamamoto, Y Kakugawa, Y Ohtake, N Saito, Y Matsumura.	Application of miRNA expression analysis on exfoliated colonocytes for colorectal cancer diagnosis.	Gastrointestinal Cancer Targets and Therapy.	2	11-18	2012
M Yasunaga, S Manabe, D Tarin, Y Matsumua.	Tailored immunoconjugate therapy depending on a quantity of tumor stroma.	Cancer Sci.	104(2)	231-237	2013
R. J. Christie, N. Nishiyama et al.	Targeted polymeric micelles for siRNA treatment of experimental cancer by intravenous injection	ACS Nano	6 (6)	5174-5189	2012
F. Pittella, N. Nishiyama et al.	Pancreatic cancer therapy by systemic administration of VEGF siRNA contained in calcium phosphate/charge-conversional polymer hybrid nanoparticles	J. Control. Release	161 (3)	868-874	2012
P. Mi, N. Nishiyama et al.	Gd-DTPA-loaded polymer-metal complex micelles with high relaxivity for MR cancer	Biomaterials	34 (2)	492-500	2013
Omata D, Negishi Y, Yamamura S, Hagiwara S, Endo-Takahashi Y, Suzuki R, Maruyama K, Nomizu M, Aramaki Y.	Involvement of Ca^{2+} and ATP in enhanced gene delivery by bubble liposomes and ultrasound exposure.	Mol. Pharm.	9	1017-1023	2012

Oda Y, Suzuki R, Otake S, Nishiie N, Hirata K, Koshima R, Nomura T, Utoguchi N, Kudo N, Tachibana K, Maruyama K.	Prophylactic immunization with Bubble liposomes and ultrasound-treated dendritic cells provided a four-fold decrease in the frequency of melanoma lung metastasis.	J. Control. Release	160	362-366	2012
S. Manabe, H. Machida, Y. Aihara, M. Yasunaga, Y. Ito	Development of Diketopiperazine-forming Dipeptidy Pro-Gly Spacer for Preparation of Antibody-Drug Conjugate	Med. Chem. Commun.	4(5)	792-796	2013

Gastrointestinal Cancer: Targets and Therapy

Dovepress

open access to scientific and medical research

Open Access Full Text Article

ORIGINAL RESEARCH

Application of miRNA expression analysis on exfoliated colonocytes for diagnosis of colorectal cancer

Satoru Murata[1]
Yoshikatsu Koga[2]
Yoshihiro Moriya[3]
Takayuki Akasu[3]
Shin Fujita[3]
Seiichiro Yamamoto[3]
Yasuo Kakugawa[4]
Yosuke Ohtake[4]
Norio Saito[1]
Yasuhiro Matsumura[2]

[1]Colorectal Surgery Division, Department of Surgical Oncology, National Cancer Center Hospital East, Kashiwa, Japan [2]Investigative Treatment Division, Research Center for Innovative Oncology, National Cancer Center Hospital East, Kashiwa, Japan [3]Department of Surgery, National Cancer Center Hospital, Tokyo, Japan [4]Cancer Screening Division, National Cancer Center Research Center for Cancer Prevention and Screening, Tokyo, Japan

Background: Several methods for the early detection of colorectal cancer to reduce its mortality rate have been reported. Here, we investigated the potential of a fecal micro RNA test for the early detection of colorectal cancer.

Methods: Patients with colorectal cancer (n = 299) and healthy volunteers (n = 116) with no abnormalities detected by screening colonoscopy were enrolled in this case-control study. Micro RNA expression in the colonocytes of patients with colorectal cancer (n = 47) and in healthy volunteers (n = 35) were analyzed in the training set, and the micro RNA expression in the colonocytes of patients with colorectal cancer (n = 252) and healthy volunteers (n = 81) was validated in the validation set.

Results: In the training study, significant differences in the relative expression level of miR-17-92 cluster, -106a, -135, and -146a were observed between patients with colorectal cancer and healthy volunteers ($P < 0.01$). The area under the receiver operating characteristic curve using miR-17, -18a, -19a, -19b, -20a, -92a, -106a, -135b, and -146a was more than 0.7. The overall sensitivity and specificity in the training study using these micro RNAs was 70.2% (33/47) and 74.3% (26/35), respectively. The overall sensitivity and specificity in the validation study was 67.5% (170/252) and 75.3% (61/81), respectively.

Conclusion: We have developed a fecal micro RNA test for exfoliated colonocytes for colorectal cancer screening. Further comparative study of this test for colorectal cancer screening is needed.

Keywords: colorectal cancer, fecal micro RNA, colonocytes, cancer screening, fecal RNA test

Introduction

The early stage of colorectal cancer is curable by surgical resection, thus a suitable colorectal cancer screening test is necessary to reduce its mortality rate. The fecal occult blood test has been used widely as a screening test for colorectal cancer.[1–3] However, large-scale studies have shown that the sensitivity of the fecal occult blood test is not very high using total colonoscopy as a reference standard in all subjects.[4–7] Therefore, several attempts for the early detection of colorectal cancer have been reported. In fecal DNA-based analysis, the stool DNA test[6] was recommended as a colorectal cancer screening method.[8] Further, we have reported several DNA-based methods for the detection of early-stage colorectal cancer using direct sequence analysis[9] and single-strand conformation polymorphism analysis[10] in exfoliated colonocytes. However, the sensitivity and specificity of the stool DNA test were insufficient compared with that of the fecal occult blood test.[11] Another technical issue was that several mutation sites of adenomatous polyposis coli (*APC*), *Kras*, and *p53* genes in colorectal cancer

Correspondence: Yasuhiro Matsumura
Investigative Treatment Division, Research Center for Innovative Oncology, National Cancer Center Hospital East, 6-5-1 Kashiwanoha, Kashiwa 277-8577, Japan
Tel +814 7134 6857
Fax +814 7134 6857
Email yhmatsum@east.ncc.go.jp

http://dx.doi.org/10.2147/GICTT.S30927

tissue were not always identical in those genes.[12] In addition, the DNA mutation analysis was complicated and expensive. This may make the use of fecal DNA analysis for colorectal cancer screening unrealistic.

Gene expression analysis based on real-time reverse transcription polymerase chain reaction (RT-PCR) has been shown to be relatively simple and cost-effective. Several attempts to detect colorectal cancer by RT-PCR in fecal samples have been reported.[13–15] In those reports, the expression analyses of *COX2* and *MMP7* in fecal RNA, and *COX2*, *MMP7*, *MYBL2*, and *TP53* in colonocyte RNA were conducted.[13,15,16]

MicroRNAs (miRNAs) are small (18–25 nucleotide) noncoding RNA molecules that regulate the activity of specific mRNA targets and play a major role in development of cancer. miRNA downregulates multiple target gene expressions by degrading mRNA or blocking its translation into protein through RNA interference.[17,18] Several miRNAs, such as miRNA-21 (miR-21), the miR-17-92 cluster and miR-135, were found to be highly expressed in colorectal cancer tissue.[19–22] Several recent studies have clarified that the circulating miRNA in plasma is a potential marker for detection of colorectal cancer,[23,24] and is remarkably stable in plasma and protected from endogenous RNase activity.[25]

We have developed a fecal miRNA test using colonocyte RNA.[26] In the present study, we analyzed several miRNAs using an optimal internal control to improve the accuracy of the fecal miRNA test. Following selection of a suitable target and threshold in the training study, the fecal miRNA test was evaluated in a validation study to determine its potential for early detection of colorectal cancer.

Materials and methods

Fecal samples and isolation of exfoliated cells

Naturally evacuated fecal samples were obtained from patients with colorectal cancer before surgical resection. Fecal samples were also obtained from healthy volunteers a few weeks after screening colonoscopy. All patients with colorectal cancer and healthy volunteers were instructed to evacuate at home into a disposable 5 × 10 cm polystyrene tray (AsOne, Osaka, Japan) and then bring the sample to the reception counter at the outpatient clinic or the Cancer Prevention and Screening Center of the National Cancer Center. The fecal samples were processed immediately after they were brought to our laboratory.

For the isolation of colonocytes from naturally evacuated feces, we used two kinds of immunomagnetic beads tagged with antihuman EpCAM monoclonal antibodies, ie, Dynabeads Epithelial Enrich (Dynal, Oslo, Norway) and JSR beads (JSR, Tsukuba, Japan).[27] The ability to isolate cells from feces using Dynal beads and JSR beads was almost same. The samples were processed as described previously.[9] Briefly, the fecal sample was homogenized with a buffer (40 mL) consisting of Hanks' solution, 10% fetal bovine serum, and 25 mM HEPES buffer (pH 7.35) at 200 rpm for one minute using a Stomacher system (Seward, Thetford, UK). The homogenate was filtered through a nylon filter (pore size, 512 μm), and following the addition of 80 μL of the immunomagnetic beads, the sample mixture was incubated for 30 minutes under gentle rolling conditions at room temperature. The mixture on the magnet was incubated on a shaking platform for 15 minutes at room temperature. The supernatant was then removed and the colonocytes in the pellet were stored at –80°C until RNA extraction.

miRNA array for selection of internal control and target miRNA

To determine the internal control for miRNA analysis and the suitable target of miRNA, the colonocyte RNA of five patients with colorectal cancer and five healthy volunteers was analyzed using the TaqMan MicroRNA Array v3.0 (Applied Biosystems, Foster, CA), in accordance with the manufacturer's instructions. RT-PCR was performed using an Applied Biosystems 7900HT fast real-time PCR system. Next, the target miRNAs were validated using total RNA extracted from both the cancer tissue and the normal mucosa of 31 patients with colorectal cancer.

Fecal miRNA analysis in patients with colorectal cancer and healthy volunteers

From August 2003 to November 2003 and from June 2004 to July 2004, 47 patients with colorectal cancer and 35 healthy volunteers were enrolled into the training study, respectively. From November 2003 to November 2009 and from July 2004 to March 2005, 252 patients with colorectal cancer and 81 healthy volunteers were enrolled in the validation study, respectively. The characteristics of these patients and volunteers are summarized in Table 1. All the patients with colorectal cancer had undergone surgical resection of their primary cancer at the National Cancer Center Hospital, Tokyo, Japan. No remarkable changes were observed except Dukes' stage classification between the training study and the validation study. All the healthy volunteers were confirmed to have no symptoms and evident abnormalities (eg, adenoma or carcinoma, including hyperplastic polyps) by screening

Table 1 Characteristics of CRC patients and healthy volunteers

Characteristics	Training set		Validation set	
	CRC patients (n = 47)	Healthy volunteers (n = 35)	CRC patients (n = 252)	Healthy volunteers (n = 81)
Age, years				
Median	62	60	63	59
Range	35–83	40–69	32–86	41–70
Sex, no (%)				
Male	33 (70.2)	19 (54.3)	162 (64.3)	33 (40.7)
Female	14 (29.8)	16 (45.7)	90 (35.7)	48 (59.3)
Tumor location, no (%)				
Cecum	2 (4.3)		17 (6.7)	
Ascending colon	7 (14.9)		39 (15.5)	
Transverse colon	2 (4.3)		15 (6.0)	
Descending colon	2 (4.3)		10 (4.0)	
Sigmoid colon	9 (19.1)		51 (20.2)	
Rectum	25 (53.2)		120 (47.6)	
Tumor size, mm				
Median	38		37	
Range	7–76		9–160	
Histology, no (%)				
W/D	21 (44.7)		143 (56.7)	
M/D	23 (48.9)		93 (36.9)	
P/D	2 (4.3)		7 (2.8)	
Mucinous carcinoma	1 (2.1)		8 (3.2)	
Carcinoid tumor			1 (0.4)	
Tumor depth, no (%)				
T1	5 (10.6)		34 (13.5)	
T2	8 (17.0)		60 (23.8)	
T3	33 (70.2)		154 (61.1)	
T4	1 (2.1)		4 (1.6)	
Dukes' stage, no (%)				
A	10 (21.3)		78 (31.0)	
B	9 (19.1)		69 (27.4)	
C	21 (44.7)		88 (34.9)	
D	7 (14.9)		17 (6.7)	

Abbreviations: CRC, colorectal cancer; W/D, well-differantiated adenocarcinoma; M/D, moderately differentiated adenocarcinoma; P/D, poorly differentiated adenocarcinoma.

colonoscopy performed at the Research Center for Cancer Prevention and Screening, National Cancer Center, Tokyo. The median age of the healthy volunteers was relatively younger than that of the patients with colorectal cancer. Regarding gender, the number of women was relatively higher among the healthy volunteers than among the patients with colorectal cancer. All participants were provided with detailed information about the study, and each gave written informed consent to participate in the study, which was approved by the institutional review board of National Cancer Center, Japan.

miRNA expression analysis using real-time PCR

Total RNA was extracted from the colonocytes isolated from the fecal samples using an miRNeasy Mini Kit (QIAGEN, Valencia, CA), and cDNA was synthesized using a TaqMan MicroRNA RT Kit (Applied Biosystems), in accordance with the manufacturer's instructions. RT-PCR was performed with precycling heat activation at 95°C for 20 seconds, followed by 40 cycles of denaturation at 95°C for 3 seconds, and annealing/extension at 60°C for 30 seconds, using an Applied Biosystems 7500 fast RT-PCR system. For the analysis of all miRNAs, we used the TaqMan microRNA assay (Applied Biosystems). miRNA expression analysis was conducted using the comparative Ct (threshold cycle) method. In this analysis, the formulae for the relative quantification of each gene were as follows: (dCt of each miRNA) = (Ct of each miRNA) − (Ct of miR-24), and (relative quantification of each miRNA) = $2^{-(\text{dCt of each miRNA})}$.

Statistical analysis

Differences in relative quantification of the miRNAs were analyzed using the two-sided Mann–Whitney *U*-test.

Statistical analyses were performed using SPSS Statistics version 19 for Windows (IBM, Tokyo, Japan). $P < 0.05$ was considered to indicate a statistically significant difference.

Results

Suitable internal control of miRNA analysis

Of 749 miRNAs, the average number of PCR-successful miRNA was 180 (range 90–295) in patients with colorectal cancer and 157 (53–242) in healthy volunteers, respectively. Forty miRNAs could be detected in all five patients with colorectal cancer and five healthy volunteers using the TaqMan MicroRNA Array, and these miRNAs served as candidates for internal control (Figure 1). Average Ct values of these miRNAs in the patients with colorectal cancer and healthy volunteers were 27.72 (23.81–31.16) and 28.78 (25.04–32.94), respectively. Mean differences in Ct values of miR-16, 24, -200c, and U6 from the average Ct values of these miRNAs were -0.12 ± 0.99, -1.48 ± 0.48, -2.57 ± 1.04, and 1.18 ± 3.19, respectively. miR-24 expression was the most stable and constant from among all miRNAs.

Selection of target miRNAs for colorectal cancer detection

According to the results of miRNA array, 20 miRNAs were selected as candidates for miRNA analysis (Table 2). Using tissue RNA, miR-17, -18a, -19a, -19b, -20a, -21, -92a, -106a, -135a, -135b, -146a, -183, -223, and -454* in cancer tissue were expressed at significantly higher levels than those in normal tissue ($P < 0.05$). On the other hand, there was no significant difference of expression for miR-34a, -155, -191, -206, -564, and -1208 between cancer tissue and normal tissue ($P > 0.1$). These 14 miRNAs were selected to target miRNAs for detection of colorectal cancer.

Relative quantification of each miRNA in colonocytes

The relative expression level of each miRNA was calculated using that of miR-24 as an internal control for 47 patients with colorectal cancer and 35 healthy volunteers in the training set (Table 1). We observed significant differences in the relative expression level of miR-17, -18a, -19a, -19b, -20a, -92a, -106a, -135a, -135b, and -146a between the patients

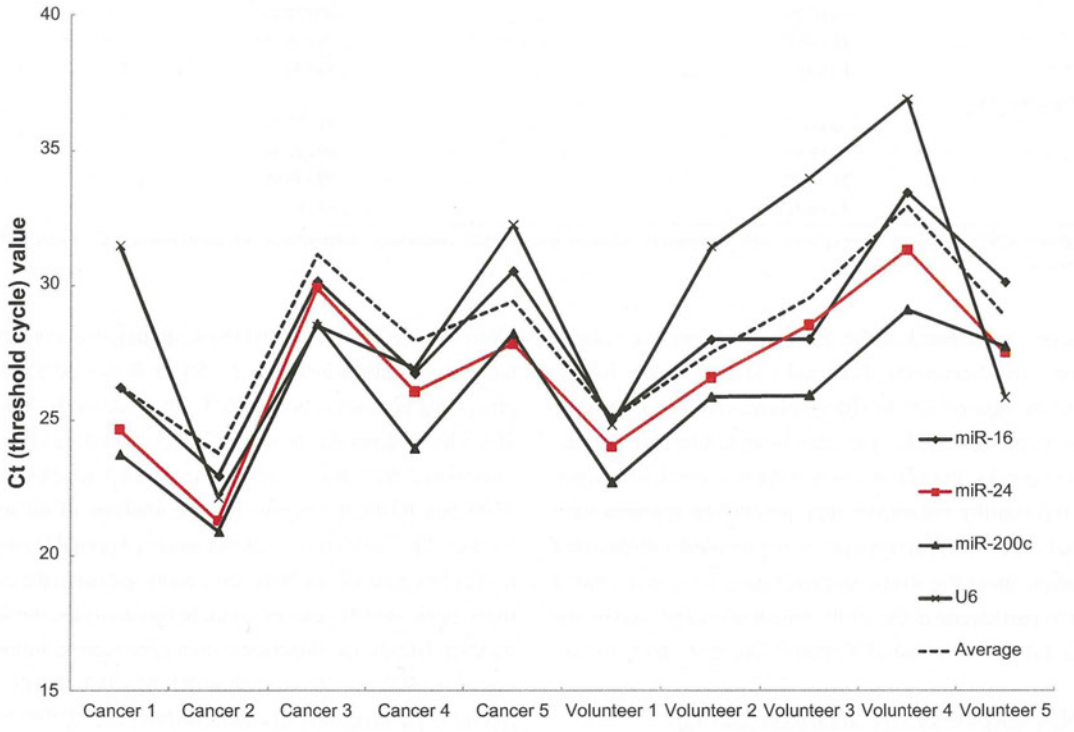

Figure 1 Ct values of candidates for internal control. Of 749 miRNAs, 40 could be detected in all of five patients with colorectal cancer and five healthy volunteers using the TaqMan MicroRNA Array.

Notes: The average Ct values of these miRNAs in patients with colorectal cancer and healthy volunteers were 27.72 (23.81–31.16) and 28.78 (25.04–32.94). The differences in the Ct values of miR-16, 24, -200c, and U6 from the average Ct values of these miRNAs were -0.12 ± 0.99 (average ± standard deviation), -1.48 ± 0.48, -2.57 ± 1.04, and 1.18 ± 3.19. The average Ct value of 40 miRNAs is indicated by the dotted line.

Abbreviations: Ct, threshold cycle; miRNA, micro RNA.

Table 2 Mean values of relative quantifications of target miRNA in tissue samples

	Colorectal cancer (n = 31)	Normal mucosa (n = 31)	*P* value
	Mean RQ (range)	Mean RQ (range)	
miR-17	1.50 (0–4.56)	0.44 (0.20–0.95)	<0.001
miR-18a	0.037 (0.002–0.135)	0.007 (0.001–0.020)	<0.001
miR-19a	0.007 (0.001–0.041)	0.002 (0–0.005)	<0.001
miR-19b	0.040 (0.002–0.164)	0.012 (0.002–0.040)	0.001
miR-20a	0.472 (0.047–1.462)	0.119 (0.026–0.284)	<0.001
miR-21	0.850 (0.190–2.239)	0.216 (0.065–0.757)	<0.001
miR-34a	0.024 (0.005–0.047)	0.023 (0.010–0.039)	0.8
miR-92a	5.117 (0.434–27.569)	1.893 (0.728–3.779)	<0.001
miR-106a	0.311 (0.092–1.187)	0.120 (0.054–0.286)	<0.001
miR-135a	0.008 (0.001–0.028)	0.001 (0–0.002)	<0.001
miR-135b	0.092 (0.014–0.330)	0.006 (0.001–0.024)	<0.001
miR-146a	0.216 (0.050–0.641)	0.139 (0.033–0.387)	0.001
miR-155	0.144 (0.038–0.431)	0.153 (0.059–0.437)	0.4
miR-183	0.012 (0.004–0.030)	0.004 (0.001–0.009)	<0.001
miR-191	0.515 (0.106–1.335)	0.485 (0.117–1.250)	0.5
miR-206	0.002 (0–0.016)	0.002 (0–0.010)	0.6
miR-223	0.416 (0.072–2.144)	0.205 (0.044–0.754)	0.006
miR-454*	0.0001 (0–0.0003)	0.0001 (0–0.0002)	0.03
miR-564	0.0003 (0–0.0025)	0.0003 (0–0.0022)	0.2
miR-1208	0.0001 (0–0.0008)	0.0002 (0–0.0028)	0.6

Notes: *P* value was analyzed by the Mann–Whitney *U*-test and $P < 0.05$ was considered to indicate a statistically significant difference.
Abbreviation: RQ, relative quantification.

with colorectal cancer and the healthy volunteers ($P < 0.01$). On the other hand, there was no significant difference in the relative expression level of miR-21, -183, -223, and -454* between the colorectal cancer patients and the healthy volunteers ($P > 0.1$, Table 3).

Area under ROC curve

The data for sensitivity and specificity calculated using relative quantifications of miRNA in patients with colorectal cancer and healthy volunteers were blotted into a receiver operating characteristic (ROC) curve (Figure 2). Areas under the ROC curve using miR-21, -135a, -183, -223, and -454* were less than 0.6. On the other hand, areas under the ROC curve using miR-17, -18a, -19a, -19b, -20a, -92a, -106a, -135b, and -146a were more than 0.7.

Sensitivity and specificity of miRNA expression analysis in training study

From the abovementioned results, we set miR-17, -18a, -19a, -19b, -20a, -92a, -106a, -135b, and -146a as a new miRNA set for detection of colorectal cancer. The thresholds of miR-17, -18a, -19a, -19b, -20a, -92a, -106a, -135b, and -146a were 2.1, 0.16, 0.57, 2.5, 1.4, 8.2, 3.2, 0.13, and 0.61, respectively (Table 4). The specificity of the healthy volunteers using each miRNA was set at 94.3% (33/35). The overall sensitivity of patients with colorectal cancer and the specificity of healthy volunteers were 70.2% (33/47, 95% confidence interval [CI] 55.1–82.7) and 74.3% (26/35, 95% CI 56.8–87.5), respectively.

Table 3 Mean values of relative quantifications of target miRNA compared with an internal control, miR-24

	CRC patients (n = 47)	Healthy volunteers (n = 35)	*P* value
	Mean RQ (range)	Mean RQ (range)	
miR-17	1.34 (0–3.76)	0.94 (0–11.85)	<0.001
miR-18a	0.12 (0–0.96)	0.04 (0–0.80)	<0.001
miR-19a	0.30 (0–1.55)	0.12 (0–1.66)	<0.001
miR-19b	1.35 (0–7.89)	0.71 (0–5.38)	<0.001
miR-20a	0.84 (0–3.56)	0.33 (0–2.13)	<0.001
miR-21	16.90 (0.28–66.49)	12.02 (0–64.94)	0.2
miR-92a	7.45 (0.38–35.02)	2.74 (0–14.05)	<0.001
miR-106a	1.26 (0–4.08)	0.78 (0–6.07)	<0.001
miR-135a	0.004 (0–0.043)	0.00002 (0–0.0006)	0.01
miR-135b	0.16 (0–2.21)	0.02 (0–0.28)	<0.001
miR-146a	0.53 (0–3.05)	0.13 (0–1.95)	<0.001
miR-183	0.010 (0–0.202)	0.009 (0–0.104)	0.5
miR-223	14.41 (1.59–49.90)	16.33 (0.03–53.63)	0.9
miR-454*	0.013 (0–0.560)	0.003 (0–0.097)	1

Notes: *P* value was analyzed by the Mann–Whitney *U*-test and $P < 0.05$ was considered to indicate a statistically significant difference.
Abbreviations: CRC, colorectal cancer; RQ, relative quantification.

Sensitivity and specificity of miRNA expression analysis in validation study

After the training study, 252 patients with colorectal cancer and 81 healthy volunteers were validated in the validation study (Table 1). The thresholds of all miRNAs for the validation study were the same as those for the training study. The overall sensitivity of the patients with colorectal cancer and the specificity of the healthy volunteers were 67.5% (170/252, 95% CI 61.3–73.2) and 75.3% (61/81, 95% CI 64.5–84.2), respectively (Table 5). There was no remarkable difference between the training study and the validation study.

Discussion

In our recent preliminary study, we analyzed the expression of miRNA in exfoliated colonocytes using oncogenic miRNAs, such as the miR-17-92 cluster, miR-21, and miR-135 normalized by U6.[26] We found that the expression analysis on the miRNA extracted from exfoliated colonocytes was feasible. In the present study, we adopted a more suitable internal control for miRNA expression and the optimal miRNA set for detecting colorectal cancer using TaqMan MicroRNA

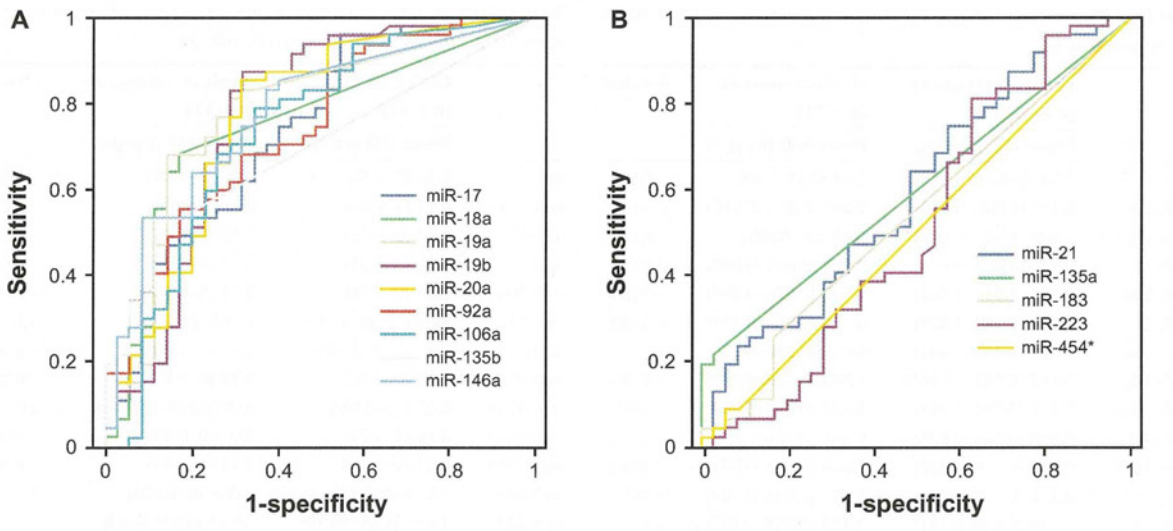

Figure 2 Areas under the ROC curve. (**A**) ROC curve using miR-17, -18a, -19a, -19b, -20a, -92a, -106a, -135b, and -146a. Area under the ROC using these miRNAs were more than 0.7. (**B**) ROC curve using miR-21, -135a, -183, -223, and -454*.
Note: Areas under the ROC curve using these miRNAs were less than 0.6.
Abbreviations: miRNA, micro RNA; ROC, receiver operating characteristic.

Array. The highly stable expression in both patients with colorectal cancer and in healthy volunteers was necessary for the internal control. Because expression of miR-24 in the colonocytes of patients with colorectal cancer and healthy volunteers was more stable and constant than that of the miR-200 family or U6 that are sometimes used as a provisional internal control, miR-24 was adopted as an internal control in the present study. However, miR-24 was not used as an internal control in previous studies. Therefore, we believe that establishment of a universal internal control for miRNA analysis is urgently needed.

The miR-17-92 cluster, -21, -34a, -106a, -135, -146a, -155, -183, -191, -206, -223, -454*, -564, and -1208 were selected from 749 miRNAs as candidates for miRNA analysis using TaqMan MicroRNA Array. Among those, the miR-17-92 cluster, -21, -106a, -135, -146a, -183, -223, and -454* were highly expressed in colorectal cancer tissue compared with the normal mucosa in our preliminary results. To date, various reports have shown that the miR-17-92 cluster, -21, -106a, -135, and -223 were expressed more strongly in colorectal cancer tissue than in normal colorectal tissue.[19–22,28–31] Though it has been shown that miR-146a is highly expressed in several types of cancer tissue,[32,33] it has been reported that miR-146a is tumor suppressor miRNA.[34] These results are controversial; however, miR-146a was expressed to a significantly greater extent in colorectal cancer tissue than in normal mucosa in our study. Thus, we decided to use miR-17-92 cluster, -21, -106a, -135, -146a, -183, -223,

Table 4 Sensitivity and specificity of each miRNA expression using optimal threshold in training set

	Threshold	CRC patients (n = 47)		Healthy volunteers (n = 35)	
		No	Sensitivity (%) (95% CI)	No	Specificity (%) (95% CI)
Combined markers		33	70.2 (55.1–82.7)	26	74.3 (56.8–87.5)
miR-17	2.1	8	17.0 (7.6–30.8)	33	94.3 (80.9–99.3)
miR-18a	0.16	11	23.4 (12.3–38.0)	33	94.3 (80.9–99.3)
miR-19a	0.57	7	14.9 (6.2–28.3)	33	94.3 (80.9–99.3)
miR-19b	2.5	6	12.8 (4.8–25.7)	33	94.3 (80.9–99.3)
miR-20a	1.4	10	21.3 (10.7–35.7)	33	94.3 (80.9–99.3)
miR-92a	8.2	15	31.9 (19.1–47.2)	33	94.3 (80.9–99.3)
miR-106a	3.2	1	2.1 (0.1–11.3)	33	94.3 (80.9–99.3)
miR-135b	0.13	13	27.7 (15.6–42.7)	33	94.3 (80.9–99.3)
miR-146a	0.61	13	27.7 (15.6–42.7)	33	94.3 (80.9–99.3)

Abbreviations: CRC, colorectal cancer; 95% CI, 95% confidence interval.

Table 5 Sensitivity and specificity of miRNA expression (validation set)

microRNA	CRC patients (n = 252)		Healthy volunteers (n = 81)	
	No	Sensitivity (%) (95% CI)	No	Specificity (%) (95% CI)
Combined markers	170	67.5 (61.3–73.2)	61	75.3 (64.5–84.2)
miR-17	26	10.3 (6.8–14.8)	77	95.1 (87.9–98.6)
miR-18a	42	16.7 (12.3–21.8)	76	93.8 (86.2–98.0)
miR-19a	3	1.2 (0.2–3.4)	81	100 (95.5–100)
miR-19b	7	2.8 (1.1–5.6)	80	98.8 (93.3–100)
miR-20a	18	7.1 (4.3–11.0)	79	97.5 (91.4–99.7)
miR-92a	124	49.2 (42.9–55.5)	78	96.3 (89.5–99.2)
miR-106a	6	2.4 (0.9–5.1)	80	98.8 (93.3–100)
miR-135b	51	20.2 (15.5–25.7)	77	95.1 (87.9–98.6)
miR-146a	27	10.7 (7.2–15.2)	77	95.1 (87.9–98.6)

Abbreviations: CRC, colorectal cancer; 95% CI, 95% confidence interval.

and -454* for colorectal cancer detection using colonocytes in the present study.

In the training study, the expressions of miR-21, -183, -223, and -454* in exfoliated colonocytes of patients with colorectal cancer were not significantly different from those of healthy volunteers. Because relative expression of miR-135a was low in both patients with colorectal cancer and healthy volunteers, the area under the ROC curve using miR-135a was under 0.6. From the present results, we determined that miR-17, -18a, -19a, -19b, -20a, -92a, -106a, -135b, and -146a were useful for detection of colorectal cancer. The sensitivity and specificity of the miRNA assay in colonocytes was 70.2% and 74.3%, respectively. These results are almost the same as those of our previous studies,[9,10,16] and we have subsequently validated the miRNA set in the validation study.

Although the rate of patients with early-stage colorectal cancer was slightly high in the validation study compared with the training study, there were no remarkable changes between the characteristics of the training study and those of the validation study. The sensitivity and specificity of the miRNA assay in the validation study was 67.56% and 75.3%, respectively. The sensitivity and specificity of the fecal miRNA test were almost the same between the training study and the validation study. Furthermore, we could not find any specific difference between miRNA expression and the clinicopathological characteristics of colorectal cancer.

In summary, the fecal miRNA test using miR-17, -18a, -19a, -19b, -20a, -92a, -106a, -135b, and -146a was found to be useful for the detection of colorectal cancer in both the training study and the validation study. The present data may warrant further comparative study between fecal occult blood test and the fecal miRNA test for colorectal cancer screening in terms of sensitivity, specificity, and cost-effectiveness.

Acknowledgment

This work was supported by a grant-in-aid for the Program for Promotion of Fundamental Studies in Health Sciences of the National Institute of Biomedical Innovation of Japan (YK); Young Scientists (B) from the Ministry of Education, Culture, Sports, Science, and Technology of Japan (YK); the Innovation Promotion Program from the New Energy and Industrial Technology Development Organization of Japan (YM); and the Japan Society for the Promotion of Science through the "Funding Program for World-Leading Innovative R and D on Science and Technology (FIRST Program)," initiated by the Council for Science and Technology Policy (YM); and National Cancer Center Research and Development Fund (YM). We thank Satoe Miyaki, Kazuya Inoue, Junko Izumisawa, Yuko Ishihara, Hiroyo Koike, Noriko F Abe, and Masae Ohmaru for their technical assistance and Kaoru Shiina for secretarial assistance.

Disclosure

The authors report no conflicts of interest in this work.

References

1. Mandel JS, Church TR, Ederer F, Bond JH. Colorectal cancer mortality: effectiveness of biennial screening for fecal occult blood. *J Natl Cancer Inst*. 1999;91(5):434–437.
2. Scholefield JH, Moss S, Sufi F, Mangham CM, Hardcastle JD. Effect of faecal occult blood screening on mortality from colorectal cancer: results from a randomised controlled trial. *Gut*. 2002;50(6):840–844.
3. Jorgensen OD, Kronborg O, Fenger C. A randomised study of screening for colorectal cancer using faecal occult blood testing: results after 13 years and seven biennial screening rounds. *Gut*. 2002;50(1):29–32.
4. Lieberman DA, Weiss DG. One-time screening for colorectal cancer with combined fecal occult-blood testing and examination of the distal colon. *N Engl J Med*. 2001;345(8):555–560.
5. Sung JJ, Chan FK, Leung WK, et al. Screening for colorectal cancer in Chinese: comparison of fecal occult blood test, flexible sigmoidoscopy, and colonoscopy. *Gastroenterology*. 2003;124(3):608–614.
6. Imperiale TF, Ransohoff DF, Itzkowitz SH, Turnbull BA, Ross ME. Fecal DNA versus fecal occult blood for colorectal-cancer screening in an average-risk population. *N Engl J Med*. 2004;351(26):2704–2714.
7. Morikawa T, Kato J, Yamaji Y, Wada R, Mitsushima T, Shiratori Y. A comparison of the immunochemical fecal occult blood test and total colonoscopy in the asymptomatic population. *Gastroenterology*. 2005;129(2):422–428.
8. Smith RA, Cokkinides V, Brawley OW. Cancer screening in the United States, 2009: a review of current American Cancer Society guidelines and issues in cancer screening. *CA Cancer J Clin*. 2009;59(1):27–41.
9. Matsushita H, Matsumura Y, Moriya Y, et al. A new method for isolating colonocytes from naturally evacuated feces and its clinical application to colorectal cancer diagnosis. *Gastroenterology*. 2005;129(6):1918–1927.

10. Onouchi S, Matsushita H, Moriya Y, et al. New method for colorectal cancer diagnosis based on SSCP analysis of DNA from exfoliated colonocytes in naturally evacuated feces. *Anticancer Res*. 2008; 28(1A):145–150.
11. Ahlquist DA, Sargent DJ, Loprinzi CL, et al. Stool DNA and occult blood testing for screen detection of colorectal neoplasia. *Ann Intern Med*. 2008;149(7):441–450.
12. Sjoblom T, Jones S, Wood LD, et al. The consensus coding sequences of human breast and colorectal cancers. *Science*. 2006;314(5797): 268–274.
13. Kanaoka S, Yoshida K, Miura N, Sugimura H, Kajimura M. Potential usefulness of detecting cyclooxygenase 2 messenger RNA in feces for colorectal cancer screening. *Gastroenterology*. 2004;127(2):422–427.
14. Leung WK, To KF, Man EP, et al. Detection of hypermethylated DNA or cyclooxygenase-2 messenger RNA in fecal samples of patients with colorectal cancer or polyps. *Am J Gastroenterol*. 2007;102(5): 1070–1076.
15. Takai T, Kanaoka S, Yoshida K, et al. Fecal cyclooxygenase 2 plus matrix metalloproteinase 7 mRNA assays as a marker for colorectal cancer screening. *Cancer Epidemiol Biomarkers Prev*. 2009;18(6): 1888–1893.
16. Koga Y, Yasunaga M, Moriya Y, et al. Detection of colorectal cancer cells from feces using quantitative real-time RT-PCR for colorectal cancer diagnosis. *Cancer Sci*. 2008;99(10):1977–1983.
17. Bartel DP. MicroRNAs: genomics, biogenesis, mechanism, and function. *Cell*. 2004;116(2):281–297.
18. Esquela-Kerscher A, Slack FJ. Oncomirs – microRNAs with a role in cancer. *Nat Rev Cancer*. 2006;6(4):259–269.
19. Yamamichi N, Shimomura R, Inada K, et al. Locked nucleic acid in situ hybridization analysis of miR-21 expression during colorectal cancer development. *Clin Cancer Res*. 2009;15(12):4009–4016.
20. Monzo M, Navarro A, Bandres E, et al. Overlapping expression of microRNAs in human embryonic colon and colorectal cancer. *Cell Res*. 2008;18(8):823–833.
21. Diosdado B, van de Wiel MA, Terhaar Sive Droste JS, et al. MiR-17-92 cluster is associated with 13q gain and c-myc expression during colorectal adenoma to adenocarcinoma progression. *Br J Cancer*. 2009;101(4):707–714.
22. Nagel R, le Sage C, Diosdado B, et al. Regulation of the adenomatous polyposis coli gene by the miR-135 family in colorectal cancer. *Cancer Res*. 2008;68(14):5795–5802.
23. Ng EK, Chong WW, Jin H, et al. Differential expression of microRNAs in plasma of patients with colorectal cancer: a potential marker for colorectal cancer screening. *Gut*. 2009;58(10):1375–1381.
24. Huang Z, Huang D, Ni S, Peng Z, Sheng W, Du X. Plasma microRNAs are promising novel biomarkers for early detection of colorectal cancer. *Int J Cancer*. 2010;127(1):118–126.
25. Mitchell PS, Parkin RK, Kroh EM, et al. Circulating microRNAs as stable blood-based markers for cancer detection. *Proc Natl Acad Sci U S A*. 2008;105(30):10513–10518.
26. Koga Y, Yasunaga M, Takahashi A, et al. MicroRNA expression profiling of exfoliated colonocytes isolated from feces for colorectal cancer screening. *Cancer Prev Res (Phila)*. 2010;3(11):1435–1442.
27. Koga Y, Yasunaga M, Katayose S, et al. Improved recovery of exfoliated colonocytes from feces using newly developed immunomagnetic beads. *Gastroenterol Res Pract*. 2008;2008:605273.
28. Valeri N, Gasparini P, Fabbri M, et al. Modulation of mismatch repair and genomic stability by miR-155. *Proc Natl Acad Sci U S A*. 2010;107(15):6982–6987.
29. Xi Y, Formentini A, Chien M, et al. Prognostic values of microRNAs in colorectal cancer. *Biomark Insights*. 2006;2:113–121.
30. Earle JS, Luthra R, Romans A, et al. Association of microRNA expression with microsatellite instability status in colorectal adenocarcinoma. *J Mol Diagn*. 2010;12(4):433–440.
31. Link A, Balaguer F, Shen Y, et al. Fecal microRNAs as novel biomarkers for colon cancer screening. *Cancer Epidemiol Biomarkers Prev*. 2010;19(7):1766–1774.
32. Williams AE, Perry MM, Moschos SA, Larner-Svensson HM, Lindsay MA. Role of miRNA-146a in the regulation of the innate immune response and cancer. *Biochem Soc Trans*. 2008;36(Pt 6):1211–1215.
33. Philippidou D, Schmitt M, Moser D, et al. Signatures of microRNAs and selected microRNA target genes in human melanoma. *Cancer Res*. 2010;70(10):4163–4173.
34. Kogo R, Mimori K, Tanaka F, Komune S, Mori M. Clinical significance of miR-146a in gastric cancer cases. *Clin Cancer Res*. 2011;17(13): 4277–4284.

Cancer Science
The official journal of the Japanese Cancer Association

Tailored immunoconjugate therapy depending on a quantity of tumor stroma

Masahiro Yasunaga,[1] Shino Manabe,[2] David Tarin[3] and Yasuhiro Matsumura[1,4]

[1]Investigative Treatment Division, Research Center for Innovative Oncology, National Cancer Center Hospital East, Kashiwa, Chiba; [2]Synthetic Cellular Chemistry Laboratory, RIKEN Advanced Science Institute, Wako, Saitama, Japan; [3]Department of Pathology, Moores/UCSD Comprehensive Cancer Center, University of California, San Diego, La Jolla, California, USA

(Received August 28, 2012/Revised October 4, 2012/Accepted October 31, 2012/Accepted manuscript online November 5, 2012/Article first published online December 16, 2012)

The purpose of this study was to clarify the appropriate combination of targeting antibody and conjugate-design of anti-tumor immunoconjugate depending on a quantity of tumor stroma. Most human solid tumors including pancreatic cancer (PC) forming hypovascular and stroma-rich tumor hinders the penetration of monoclonal antibodies (mAbs) into the cells, and that leads to failure of the conventional cell-targeting immunoconjugate strategy. To overcome this drawback, SN-38 as topoisomerase 1 inhibitor was conjugated to a mAb to collagen 4, a plentiful component of the tumor stroma via ester-bond. The immunoconjugate, which was able to release SN-38 in physiological condition outside the cells, was effective to stroma-rich PC-tumor. On the other hand, anti-CD 20 mAb-PEG-SN-38 via carbamate-bond as conventional immunoconjugate, enabled SN-38 to be released by a carboxylesterase inside of the tumor cell following the internalization, showed strong anti-tumor activity against malignant lymphoma as hypervascular and stroma-poor tumor. The conjugate-design, in parallel with the choice of targeting antibodies, should be selected to maximize the therapeutic effect in each individual tumor having a distinct stromal structure. (*Cancer Sci* 2013; 104: 231–237)

Monoclonal antibody (mAb), which can target the tumor cell actively by the specific binding ability against corresponding antigen, easily extravasates from leaky tumor vessels but not from normal vessels, is long retained in the tumor by using active targeting and passive targeting based on the enhanced permeability and retention (EPR) effect.[1–4] Therefore, numerous mAbs have been developed and conjugated with anticancer agents (ACAs) or toxins to create an "immunoconjugate strategy".[5–8] Recent examples of the conjugates include anti-CD33 immunoconjugate-calicheamicin and anti-CD20 radiolabeled immunoconjugate, were effective to hematological malignancy such as malignant lymphoma and leukemia.[5] Heterogeneity of the tumor cells, however, prevents development of the immunoconjugate chemotherapy based on cell-specific antigen.[9–12] Moreover, conventional immunoconjugates depend on cleavage of conjugation site with intracellular biochemical (enzymatic) process after the cell-uptake of the conjugate.[13–16] In addition to such annoying characteristics of cancer cells themselves, most human solid tumors such as pancreatic cancer and gastric cancer, possess abundant stroma that hinders the distribution of mAbs (Fig. 1a).[17–20] To overcome these drawbacks, we developed a unique strategy whereby the cancer-stromal targeting (CAST) therapy by cytotoxic immunoconjugate bound to the collagen 4 or fibrin network in the tumor stroma, from which the payload released gradually and distributed throughout the tumor, resulting in the arrest of tumor growth due to induced damage to tumor cells and tumor vessels.[21,22] Besides, there have been a few reports describing tumor stromal targetingimmunoconjugates, a mAb against a cell surface antigen FAP as fibroblast targeting therapy, or a mAb against fibronectin for the targeting of tumor vascular endothelial cell in photodynamic therapy.[23,24] However, the merits and drawbacks of anti-stromal targeting immunoconjugate therapy in relation to the conjugate-design and the amount of tumor stroma have not yet been fully elucidated.

The purpose of this study was to clarify the appropriate combination of targeting antibody and conjugate-design of anti-tumor immunoconjugate depending on the quantity of tumor stroma. Hence, we selected two types of conjugate linker: ester-bond and carbamate-bond. We hypothesized that a combination of anti-stromal targeting mAb and a linker composed of ester-bond to release ACA outside the cells would be effective against the stroma-rich cancer. Conversely, anti-cancer cell targeting via carbamate-bond to release ACA inside the cells would be effective against stroma-poor cancer. It seemed that the outcome of immunoconjugate therapy against each individual tumor having distinct stromal structure was dependent on the selection of conjugation-design, as well as targeting mAb.

Materials and Methods

Antibodies and cells. Anti-EpCAM (B8-4) and Anti-collagen 4 antibody (35-4) were prepared as previously reported.[21] Anti-human CD20 antibody (rituximab) was purchased from Daiichi-Sankyo (Tokyo, Japan). Human malignant lymphoma cell line RL was purchased from the American Type Culture Collection (Rockville, MD, USA). Human PC cell line SUIT2 was purchased from the Health Science Research Resources Bank (Osaka, Japan).

***In vivo* imaging and immunohistochemistry.** Immunohistochemistry was conducted using anti CD31 antibody (R&D Systems, Minneapolis, MN, USA), anti-collagen 4 antibody and anti-CD20 (rituximab), or anti-EpCAM antibody as first antibodies, Alexa 488-, 555- or 647-labeled anti-human, mouse, rat or goat IgG (Invitrogen, Carlsbad, CA, USA) as second antibodies.

For mouse-systemic *in vivo* imaging or tracking of antibody in the tissue, IRDye 800 (Li-Cor Biosciences, Lincoln, NE, USA) alexa-647 (Invitrogen) or Qdot 625 (Invitrogen) labeled antibodies were injected into the mice tail vein at 100 μg /body. Fluorescence images were obtained using OV110 (Olympus, Tokyo, Japan), BZ-9000 (Keyence, Osaka, Japan), LSM 710 (Carl Zeiss, LinkedIn Germany).

Immunoconjugate. The detailed process of chemical synthesis is shown in the Data S1. The final structure was composed of one maleimide for attachment of mAb, one PEG_{12} (MW 865) spacer and one PEG_{27} (MW 1422) ester-bond or

[4]To whom correspondence should be addressed.
E-mail: yhmatsum@east.ncc.go.jp

doi: 10.1111/cas.12062

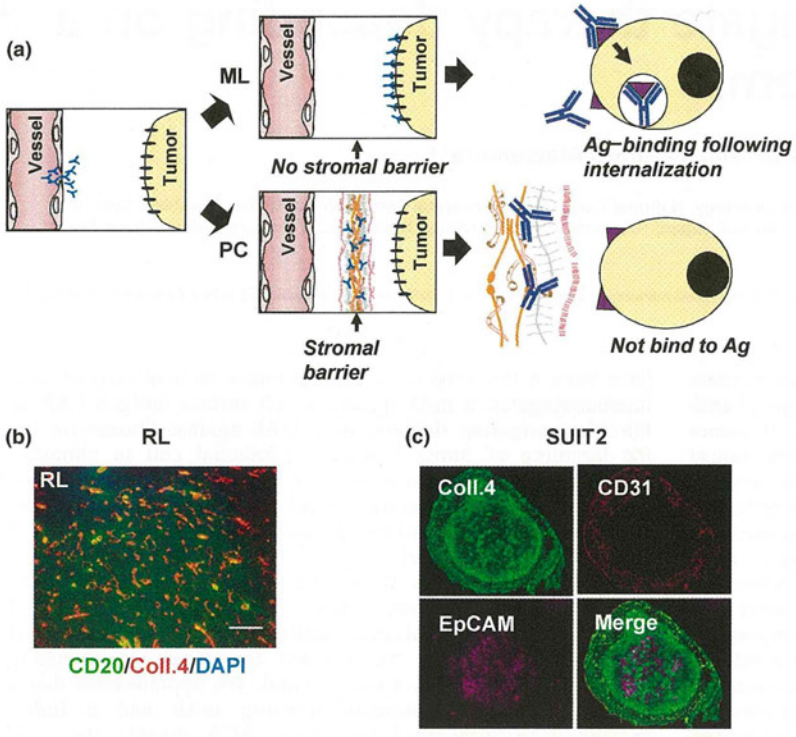

Fig. 1. The difference of tumor tissue stromal component as stromal barrier between malignant lymphoma and pancreatic cancer. (a) The schema of antibody delivery into the tumor cells. In the tumor having no stromal barrier like malignant lymphoma (ML), antibodies were delivered into the cancer cells, and can be internalized after antigen-binding. However, many human solid tumors including pancreatic cancer (PC) possess stromal barrier hindering the distribution of the immunoconjugates into cancer cells such that antigen-binding following antibody-intrernalization never occur. Ag, Antigen. (b) RL-tumor (ML) was stained with anti-CD20 (green), anti-collagen 4 (red) mAb and 4′6′-diamidino-2-phenylindole dihydrochloride (DAPI) (blue). Scale bar: 100 μm. (c) SUIT2-tumor (PC) was stained with anti-EpCAM (purple), anti-collagen 4 (green) and anti-CD31 (red) mAb. Co-existence of collagen 4 and CD 31 (yellow in Merge). Coll., collagen.

carbamate-bond for attachment of one SN-38 molecule. Interchain disulfides of the antibodies were reduced with 10 mM DTT (Sigma).[14] The numbers of free thiols were quantified with dinitrothiocyanobenzene (DNTB, Wako, Osaka, Japan). Reduced antibodies were reacted with maleimide-linker-SN-38 prodrugs in PBS containing 5 mM EDTA (pH 6) at room temperature for 1 h, then at 4°C overnight. The concentration of antibody-prodrug conjugates was determined using the Bradford method (Bio-Rad Protein Assay, 500-0006JA, Bio-Rad, Hercules, CA, USA). The numbers of residual thiols were quantified with dNTP. Each drug (SN-38)/antibody ratio was determined by comparing the numbers of free and residual thiols. In the characterization of the conjugates, statistical analysis was performed using Student's *t*-test.

Animal model and anti-tumor effects. Female BALB/c nude mice (5 weeks old) were purchased from SLC Japan (Shizuoka, Japan). Mice were inoculated subcutaneously in the flank with 5×10^6 cells of RL, or 2×10^6 of SUIT2. The length (L) and width (W) of tumor masses and body weight were measured every 4 days, and tumor volume was calculated using $(L \times W^2)/2$. All animal procedures were performed in compliance with the Guidelines for the Care and Use of Experimental Animals established by the Committee for Animal Experimental of the National Cancer Center. These guidelines meet the ethical standards required by law and also comply with the guidelines for the use of experimental animals in Japan. When the mean tumor volume reached approximately 140 mm^3 (RL) and approximately 70 mm^3 (SUIT2), mice were randomly divided into groups consisting of five mice. Immunoconjugates were administered on day 0 by the mice tail vein injection. The injection doses of antibody-SN-38 prodrug equal to an SN-38 dose of 3 mg/kg were determined by calculations based on drug (SN-38)/antibody ratio (range from 2629.08 to 3296.16 mg SN-38 per 1 mM antibody) for each drug. Statistical analysis was performed using ANOVA.

Biochemistry and hematological examination. Blood samples were taken from the healthy mice at 7 days after i.v. administration of immunoconjugates (at an equivalent SN-38 dose of 3 mg/kg). Hemograms were measured by using an auto-analyzer Celltacα MEK6358 (Nihon Kohden, Tokyo, Japan), and blood chemistry examinations were carried out by Nagahama LSL (Shiga, Japan).

Anti-collagen antibody induced arthritis. Female DBA/1J mice (5 weeks old) were purchased from SLC Japan. Anti-collagen 2 antibody (Chondrex, Redmond, WA, USA) or anti-collagen 4 antibody (clone 35-4, the same mAb in the immunoconjugate) were intraperitoneally administered on day 0 at 2 mg. Fifty micrograms of LPS (Chondrex) was intraperitoneally injected on day 3.

Results

Difference of tumor stromal component between malignant lymphoma and pancreatic cancer. We first examined the difference of the stromal component influencing the drug delivery between malignant lymphoma RL and pancreatic cancer SUIT2. Anti-CD20- or anti-EpCAM-mAb, which is specific to lymphoma or epithelial carcinoma, respectively, was used as cancer cell-specific mAb.[5,25] Anti-collagen 4 mAb was prepared to evaluate the stromal component. RL tumor consisted of CD20-positive tumor cells and collagen-4-positive blood vessels, which was stained fine-linearly but not interspersed-fibrously like the intercellular-stroma (Fig. 1b). On the other hand, SUIT2-tumor reported as the histopathology relatively resembling original human pancreatic cancer,[21,26] consisted of EpCAM-positive cancer-cells and collagen-4-positive extracellular component, the latter was composed of both CD31-positive blood vessel wall (yellow in Merge, Fig. 1c) and high amount of CD31-negative stroma (green in Merge, Fig. 1c).

Internalization and biodistribution of mAbs against malignant lymphoma or pancreatic cancer. Cell-uptake of fluorescent anti-CD20- or anti-EpCAM-mAb against RL cells or SUIT2 cells was evaluated, respectively. Anti-CD20 mAb was internalized and colocalized with intracellular lysosome in RL cells at 12 h after the incubation. On the other hand, anti-EpCAM mAbs, the majority of which was still retained on cell-surface

doi: 10.1111/cas.12062

membrane of SUIT2 cells, was poorly internalized at the same period (Fig. 2a). We next investigated the kinetics of entry of three mAbs into the tumors using an *in vivo* imaging system with near infrared fluorescence, which can provide deep tissue imaging with high fidelity.[27,28] Until day 3, all fluorescent-mAbs were delivered and retained both in RL-tumor, and SUIT2-tumor, indicating passive targeting (Fig. 2b). On Day 7, anti-EpCAM mAb in RL-tumor and anti-CD20 mAb in SUIT-2-tumor as a negative control, were almost eliminated, but anti-CD20 mAb in RL-tumor, anti-EpCAM mAb in PC-tumor and anti-collagen 4 mAb in both RL-tumor and SUIT-2-tumor were still retained in each tumor, indicating active targeting, that is, binding to their respective antigens within the lesion. There were also clear differences in the degree of intratumor accumulation among three mAbs. Anti-CD20 mAb accumulation was higher in RL-tumors than anti-EpCAM mAb in SUIT2-tumors (Fig. 2b). On the other hand anti-collagen 4 mAb accumulation was higher in SUIT2-tumors than in RL-tumors (Fig. 2b). We then examined the histological distribution of mAbs in each tumor. In RL tumor, fluorescent anti-CD20 mAb was distributed in the whole tumor area and bound to the cancer cells (Fig. 2c). Qdot-labeling system detecting lower fluorescent signals in SUIT-2 tumor was conducted to evaluate the biodistribution of each mAb. The quantity of anti-CD20 mAb observed in SUIT2 tumor was small (Fig. 2d). Anti-EpCAM mAb was observed mainly around the tumor cell-abundant area, in which collagen 4 was negative (Fig. 2d). In contrast, anti-collagen 4 mAb was mainly observed in collagen 4-positive stroma, and rarely in the tumor cell-abundant area (Fig. 2d). Thus, we succeeded in preparing three mAbs: anti-CD 20 mAb for cell-targeting against RL tumor, anti-EpCAM mAb for cell-targeting against SUIT2-tumor, and anti-collagen 4 mAb for stroma-targeting against both tumors. These three mAbs can selectively exit the vascular system through the leaky tumor vessels and distribute within each tumor according to the nature of tissue component.

Preparation and characterization of cell-targeting or stroma-targeting Immunoconjugate-PEG-SN-38 via a carbamate-bond or ester-bond. To specify the appropriate immunoconjugatge therapy against malignant lymphoma or pancreatic cancer, we prepared two types of the conjugates, one being mAb-PEG-SN-38 via a carbamate-bond[29] (Fig. 3a) and another being mAb-PEG-SN-38 via an ester-bond[21,22] (Fig. 3b). Consequently, six types of immunoconjugates, anti-CD20, anti-EpCAM or anti-collagen 4 mAb- SN-38 via a carbamate-bond or an ester-bond, were obtained. The average number of conjugated SN-38 per one mAb (drugs/mAb), ranging from 7.0 to 8.5, was shown in Figure 3c. There was no clear loss of antigen-binding activity of each mAb after the conjugation (Fig. 3D). An *in vitro* release experiment, both bonds can be cut by a carboxylesterase localized in cytoplasm to release SN-38 inside various cells (Fig. 3e). However, in physiological conditions (non-enzymatic hydrolysis), the immunoconjugate prepared via an ester-bond can release SN-38 gradually and effectively. In contrast, the immunoconjugate via a carbamate-bond cannot release SN-38 effectively in the conditions outside the cells (Fig. 3e). We then evaluated the release profiles of SN-38 from both types of immunoconjugate in mouse blood, which contained high amounts of carboxylesterase.[30] *In vivo* analysis of mouse plasma, the concentration of unbound SN-38 or bound and unbound of SN-38 from the immunoconjugate via an ester-bond or a carbamate-bond at 72 h after the mice tail vein injection were shown. Most of the immunoconjugates in the mouse blood were protected from the enzymatic cleavage (Fig. 3f). Next, we examined the difference between carbamate-bond and ester-bond in combination with cell-targeting or stromal-targeting antibody by the cytotoxicity assay. In RL cells, anti-CD 20 immunoconjugate via carbamate-bond showed strong cytotoxicity

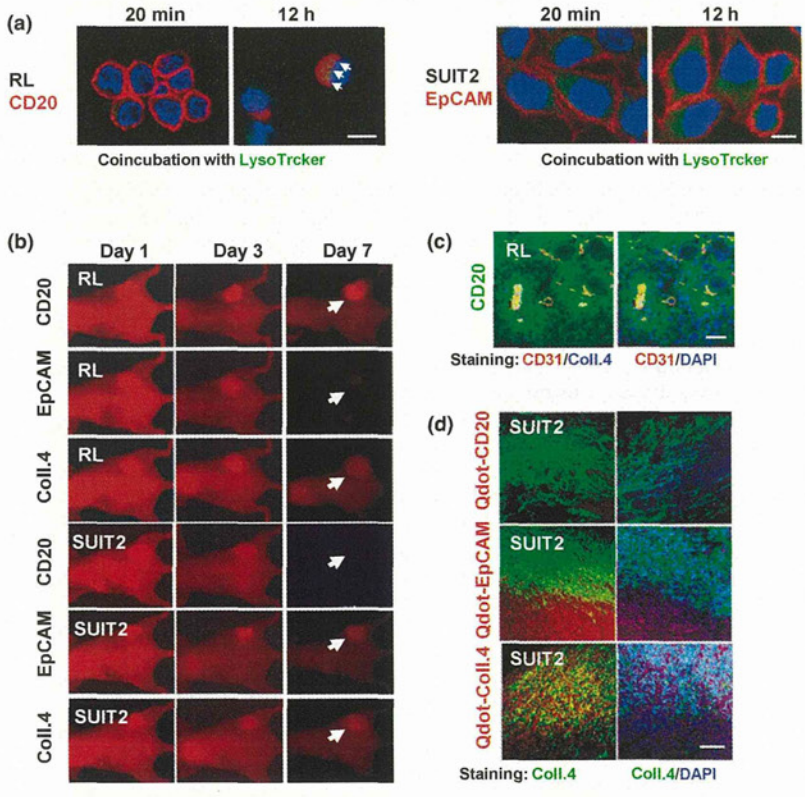

Fig. 2. Internalization and biodistribution of anti-CD20, anti-EpCAM monoclonal antibody (mAb) and anti-collagen 4 mAb. (a) Internalization of Alexafluor-633-anti-CD20 or anti-EpCAM mAb (Red) on RL or SUIT2 cells was examined at 20 min or 12 h after the incubation. Arrow shows merged yellow as co-localization with lysostracker (Green). Scale bar: 10μm. (b) *In vivo* imaging analysis of RL-, SUIT2-tumor was conducted using near-infrared labeled anti-CD20, EpCAM and collagen 4 mAbs on days 1, 3 and 7 after injection. Arrows indicate each tumor position. (c) The intra-RL-tumor distribution of Alexa 647 (green)-labeled anti-CD20 mAb was examined by confocal laser scanning microscopy at 24 h after injection. CD31 (red), Collagen 4 (blue, left panel) and nuclei (blue, right panel) were stained by immunohistochemistry or DAPI. Scale bar: 100 μm. (d) The intra-SUIT2-tumor distribution of each Qdot (red)-labeled antibody was examined by confocal laser scanning microscopy on day 7 after injection. Collagen 4 (green) or nuclei (blue) were stained by immunohisochemisty or DAPI. Scale bar: 100 μm.

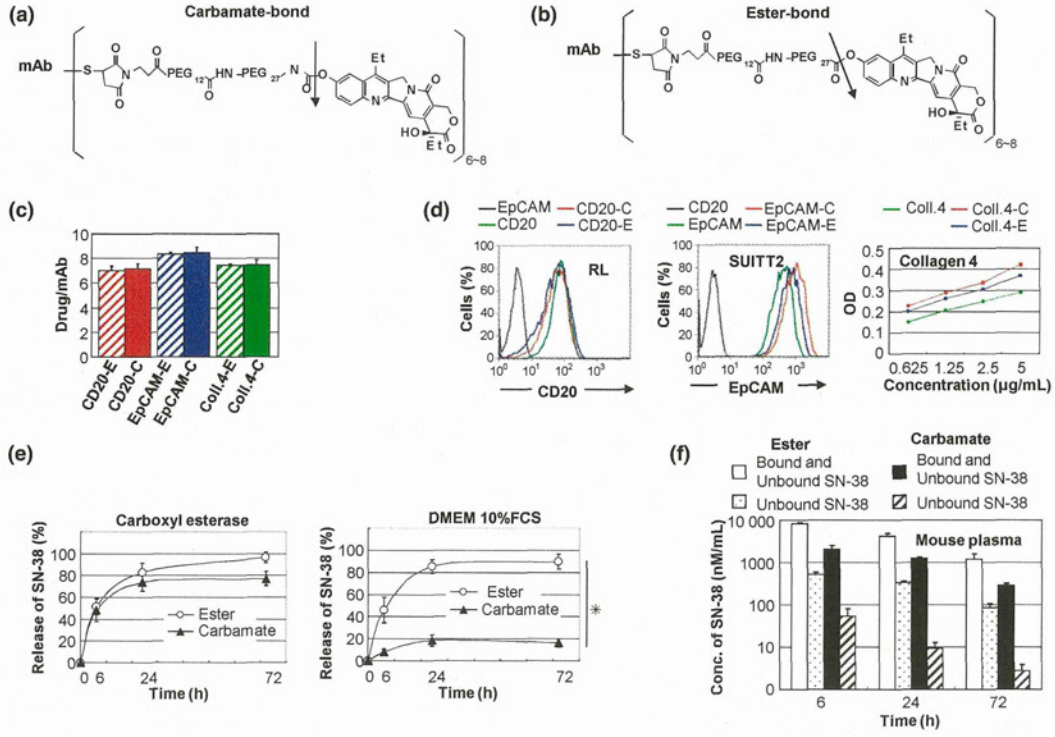

Fig. 3. Preparation and characterization of two types of immunoconjugqates-PEG-SN-38 via carbamate-bond and eser-bond. (a,b) Drug design of two types of immunoconjugates; monoclonal antibody (mAb) -PEG-SN-38 via carbamate-bond (a) and mAb-PEG-SN-38 via ester-bond (b). One antibody bears six to eight molecules of SN-38. The arrow indicates the cleavage site for releasing free active SN-38. (c)The average number of conjugated SN-38 per one mAb was shown (n = 3). Bar = standard deviation (SD). (d) Antigen-binding activity of the mAb before and after the conjugation was shown. Anti-CD 20 and EpCAM mAb were examined by fluorescence-activated cell sorting (FACS) analysis using RL cells and SUIT2 cells, respectively. Anti-collagen 4 mAb was examined by enzyme linked immunosorbent assay (ELISA) using purified protein. (e) *In vitro* release of SN-38 from two types of immunoconjugates in carboxylesterase-contained solution (left) and Dulbecco's modified eagle medium (DMEM) 10% fetal calf serum (FCS) (right) (n = 3). Bar standard deviation (SD), *P < 0.05. (f) Concentration of bound and unbound form of SN-38, and unbound form of SN-38 from two types of immunoconjugates in the mouse plasma at 6, 24, 72 h after the mice tail vein injection, were shown (n = 3). Concentrations of SN-38 were determined by high performance liquid chromatography (HPLC). Bar = standard deviation (SD).

compared with anti-CD 20 immunoconjugate via ester-bond significantly. In SUIT2 cells, although there was no significant difference, anti-EpCAM immunoconjugate via carbamate-bond had a lower tendency in the cytotoxic effect compared to anti-EpCAM immunoconjugate via ester-bond. Anti-collagen 4 immunoconjugate via ester-bond showed higher cytotoxic activity than anti-collagen 4 immunoconjugate via carbamate-bond in both cells significantly (Table 1). These results indicated that a carbamate-bond was useful for the immunoconjugate linker to work inside of the cells and an ester-bond to work outside the cells.

Cell-targeting or stroma-targeting immunoconjugate-PEG-SN-38 via carbamate-bond or ester-bond differs drastically in their anti-tumor effects depending on tumor stromal component in mice. Three mAbs conjugated with SN-38 via carbamate-bond or ester-bond (administered once, at an equivalent SN-38 dose of 3 mg/kg) were evaluated in order to know their anti-tumor effects in RL (CD20-positive stroma-poor human malignant lymphoma), SUIT2 (EpCAM-positive stroma-rich human pancreatic tumor). In RL lymphomas, cell-targeting anti-CD20 mAb- SN-38 via carbamate-bond showed superior anti-tumor activity compared to anti-CD20 mAb- SN-38 via ester-bond after the treatment (Fig. 4a). Stroma-targeting anti-collagen 4 mAb- SN-38 via ester-bond showed significant superior anti-tumor activity as compared to saline as control, but inferior to anti-CD20 mAb- SN-38 via carbamate-bond (Fig. 4a). On the contrary to RL tumor, in SUIT2 tumor, the most potent anti-tumor activity was obtained by the stroma-targeting anti-collagen 4 mAb- SN-38 via ester-bond (Fig. 4b). However, there was no significant difference in anti-tumor activity between anti-EpCAM mAb- SN-38 via carbamate-bond and via ester-bond, whereas the anti-tumor activity of anti-collagen 4 mAb- SN-38 via carbamate-bond was inferior to that of anti-collagen 4 mAb- SN-38 via ester-bond (Fig. 4b). These results clearly indicated that, in

Table 1. IC50 of free SN-38 and SN-38 conjugated to monoclonal antibody (mAb) (immunoconjugate) for malignant lymphoma and pancreatic cancer cell lines (WST-8 assay)

Malignant lymphoma cell lines	Free SN-38	SN-38 conjugated to mAb	
		CD20	Collagen 4
		Ester *vs* carbamate	Ester *vs* carbamate
RL	4.6 ± 3.7	8.7 ± 2.9 *vs* 2.1 ± 1.0*	34 ± 17 *vs* 90 ± 30*
Pancreatic cancer cell lines	**Free SN-38**	**SN-38 conjugated to mAb**	
		EpCAM	Collagen 4
		Ester *vs* carbamate	Ester *vs* carbamate
SUIT2	7.8 ± 3.6	24 ± 13 *vs* 15 ± 9	29 ± 15 *vs* 75 ± 22*

IC50 (50% cell survival) (nM), Mean ± standard deviation (n = 3), *P < 0.05.

doi: 10.1111/cas.12062

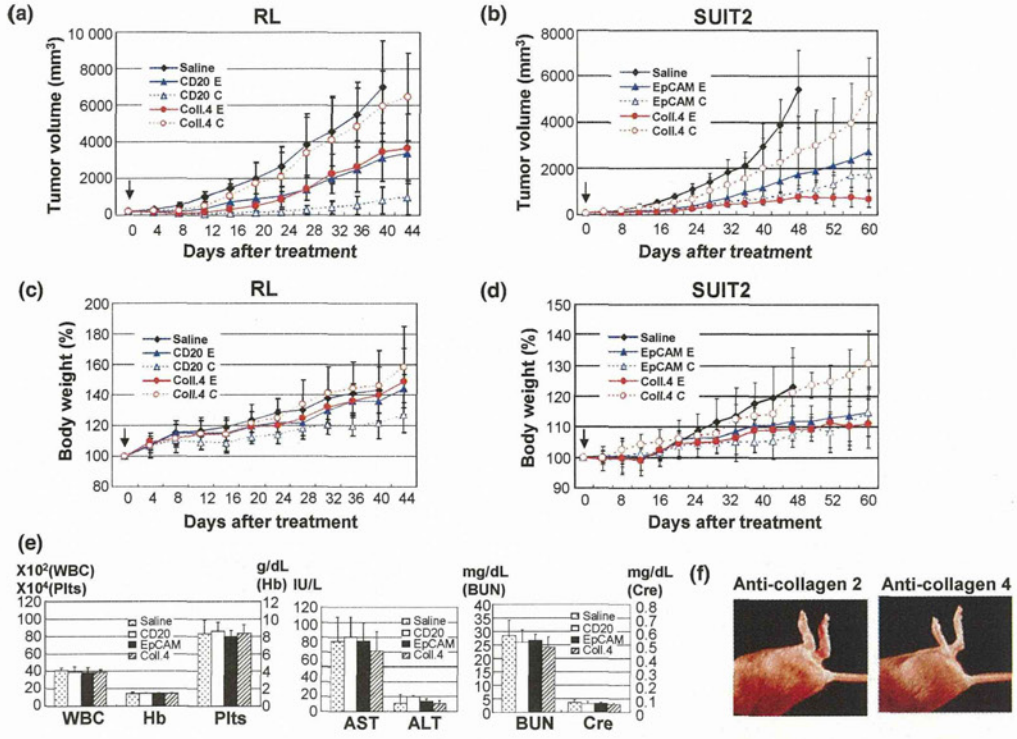

Fig. 4. Antitumor effects and toxicities of immunoconjugates-PEG-SN-38 in the combinations of anti-cell or anti-stroma targeting, carbonate-bond or ester-bond. (a,b) Anti-tumor activities and (c,d) percent changes of body weight were examined. In animal models of RL (a,c) and SUIT2 (b,d), the six types of immunoconjugates (combined anti-CD20 monoclonal antibody (mAb) =CD20, anti-EpCAM mAb=EpCAM or anti-collagen 4 mAb=Coll.4 and ester-bond=E or carbamate-bond=C), or saline as control, were administered once at an equivalent SN-38 dose of 3 mg/kg to separate groups of mice (n = 5) by intravenous bolus injection to the mice on day 0. Arrows indicate day of administration and the curves illustrate the effect of treatment on tumor size. $P < 0.0001$ (saline versus CD20-E or CD20-C, CD20-C versus CD20-E, Coll.4-E or Coll.4-C in RL tumor; saline versus EpCAM-E, EpCAM-C or Coll.4-E, Coll.4-E versus EpCAM-C or Coll.4-C, EpCAM-C versus Coll.4-C in SUIT2 tumor), $P < 0.001$ (Saline versus Coll.4-E in RL tumor; saline versus Coll.4-C, Coll.4-E versus EpCAM-E in SUIT2 tumor). Bar = standard deviation (SD). (e) Hematological (WBC, Hb and Plts) and biochemical (aspartate aminotransferase [AST], alanine aminotransferase [ALT], blood urea nitrogen [BUN] and creatinine [Cre]) examination were conducted at 7 days after i.v. administration of immunoconjugates via ester-bond or saline as control. Bar = standard deviation (SD). (f) Anti-collagen antibody induced arthritis in DBA/1J mice. The arthritis was admitted on day 7 only after the administration of anti-collagen 2 (left) but not anti-collagen 4 (right) antibodies.

stroma-poor solid tumors like malignant lymphoma, cytotoxic immunoconjugate should target to the tumor cell surface and ACA should be conjugated to mAb through carbamate-bond, which can be specifically cut by a carboxylesterase inside the tumor cell after the internalization. On the other hand, in stroma-rich tumors, the immunoconjugate should target to the stroma within tumor tissue and ACA should be attached to the mAb via ester-bond, which can be cut gradually outside the tumor cell following the accumulation of the cytotoxic immunoconjugate in the tumor stroma. It is remarkable that the feature of tumor stromal component influence the outcome of the two types of immunoconjugation drugs, cell-targeting mAb-PEG-SN-38 via carbamate-bond, or stroma-targeting mAb-PEG-SN-38 via ester-bond.

Regarding normal tissue distribution and elimination of antibodies and SN-38, there was no difference among immunoconjugates on day 7 after the administration. The dose in this study did not cause significant toxicity as shown by the change of mouse body weight (Fig. 4c,d). Moreover, there was no hepatotoxicity, nephrotoxicity, or bone marrow toxicity in mice treated with all three immunoconjugates as compared to controls (Fig. 4e). In addition, no autoimmune disease-like adverse effects such as arthritis and nephritis were observed in the administration of anti-collagen 4 mAb, whereas anti-collagen 2 mAb combined with lipopolysaccharide caused severe arthritis (Fig. 4f).

Discussion

Conventional immunoconjugate is composed of cell-targeting mAb, ACA as payload and linker for the conjugation. The linker technology is an important part of the immunoconjugate strategy, and various linkers have been exploited to date. Among them, acid labile hydrazine linkage, thiol reduction of disulfide linkers, and lysosomal peptidase proteolysis of peptide linkers were favorably applied to ensure stability in blood.[6–8] For these types of linkers, cell-mediated endocytosis of antibody (antibody-internalization) and intracellular biochemical (enzymatic) processing of the immunoconjugate were indispensable to make the active ACA work. Our carbamate-bond based linker, which is used in a clinically approved anticancer prodrug CPT-11 to release an active component SN-38 within the tumor cell but not in blood circulation[29,31,32] can be classified into the conventional type mentioned above. Anti-CD 20 Immunoconjugate-PEG-SN-38 via carbamate-bond showed strong anti-tumor activity against malignant lymphoma, in which the distribution within the tumor tissue and antibody-internalization into tumor cells occur effectively. Although there were negative reports concerning the internalization of anti-CD20 mAbs, several authors, recently demonstrated internalization of anti-CD20 mAbs including rituximab in malignant lymphoma and leukemia cells.[33–36] These conflicting results might reflect

the differences of cell types, mAbs or methodologies used.[35,36] In contrast to malignant lymphoma, most human solid tumors possess abundant stroma that hinders the tissue-distribution of antibodies.[17–22] Cell–cell interaction between malignant epithelial cells also inhibits the penetration of mAb besides tumor-stroma.[18,37] Moreover, heterogeneity of the cells in the tumor prevents development of immunoconjugate therapy based on cancer cell-specific antigen.[9–12] This led us to design an anti-stromal targeting immunoconjugate strategy using the tumor stroma both as a scaffold for binding and assembling immunoconjugates and as a relay base for a second attack by payload-ACA persistently released from the scaffold.[21,22] In this drug design we selected a specially selected linker using ester-bond, which can release SN-38 in physiological condition (non-enzymatic hydrolysis) outside the cells. Both ester-bond and carbamate-bond were concerned to be cleaved by plasma carboxyl-esterase in the circulation after the injection. Cleavages of our conjugates were very low in mouse plasma, which has much higher levels of carboxyl-esterase activity than in human.[30] Recently, we conducted clinical trials of NK012, a SN-38 incorporating polymeric micelle. In this formulation, SN-38 was conjugated to poly-Glu-chain via ester-bond. From these trials, we learned that human blood also contains high amounts of carboxylesterase. Nevertheless, NK012 proved good stability in human blood circulation.[38,39]

Anti-collagen 4 immunoconjugate exiting from vessel can bind to the outer vessel wall and cells surrounding the stroma. Anti-collagen 4 immunoconjugate via carbamate-bond was not useful because it can scarcely release SN-38 outside the cells. On the other hand, anti-collagen 4 immunoconjugate via ester-bond can release SN-38 on the stroma. Low molecular weight agent SN-38 can penetrate through stroma into the cells. SN-38 released from the scaffold of adjacent collagen-4-positive vascular wall also attack tumor endothelium.[21] Anti-collagen 4 mAb-SN-38 via ester-bond exerted more potent antitumor activity compared to anti-EpCAM mAb-SN-38 via carbamate-bond or ester-bond. It is too complicated to explain these data. However, we speculate that in addition to the insufficient attainability of anti-EpCAM mAb to tumor cells by stromal barrier and its low internalization into the cells, the retention of anti-EpCAM mAb within the tumor cell lesion is lower than that of anti-collagen 4 mAb within the tumor stroma. Consequently, the amount of SN-38 released inside of the cells from anti-EpCAM mAb-SN-38 via carbamate-bond or outside of the cells from anti-EpCAM mAb-SN-38 via ester-bond, may be less than that of SN-38 released outside of the cells from anti-collagen 4 mAb-SN-38 via ester-bond.

Although there had been a concern about the influence of anti-collagen 4 immunoconjugate on normal tissues having high level of collagen 4, we observed the safety of the immunoconjugate in several mouse models. We think that cancer stromal targeting (CAST) therapy is dependent on the fundamental concept that antibodies or immunoconjugates are generally too large to pass through the normal vessel walls, whereas they can extravasate from leaky tumor vessels to achieve tumor selective targeting by using EPR effect and bind to collagen 4, a plentiful component of the tumor stroma.[1–4,40] We also speculate that such a passive targeting effect is one of the reasons why recent anti-EGFR antibody therapies show no serious adverse effects in spite of high level EGFR expression in normal tissues including intestinal mucosa, dermis and others.[9,10,41]

In general, human cancer is classified into three types according to the tissue component. One is hypervascular stroma-poor tumor such as malignant lymphoma, the second is hypovascular stroma-rich tumor such as pancreatic cancer and stomach cancer, and the third is intermediated tumor between the two types such as breast cancer and colorectal cancer. We thus propose the new therapeutic strategy of immunoconjugates to the feature of individual tumor as tissue stromal component: (i) cell-targeting mAb conjugated with ACAs via carbamate-bond for hypervascular and stroma-poor tumor; (ii) stroma-targeting mAb conjugated with ACAs via ester-bond for hypovascular and stroma-rich tumor; (iii) both cell-targeting immunoconjugate via carbamate-bond and stroma-tgargeting via ester-bond for intermediated type of tumor (Fig. 5).

Acknowledgments

This work was supported by the Funding Program for World-Leading Innovative R&D on Science and Technology (FIRST Program) (YM), Third Term Comprehensive Control Research for Cancer from the Ministry of Health, Labour and Welfare of Japan (YM), a Grant-in-Aid for Scientific Research or Priority Areas from the Ministry of Education, Culture, Sports, Science and Technology, the Princess Takamatsu Cancer Research Fund (YM), Japanese Foundation for Multidisciplinary Treatment of Cancer (YM), Japanese Foundation for Promotion of Cancer Research (MY), National Cancer Center Research and Development Fund (MY), the Grant-in-Aid for Scientific Research from Japan Society for the Promotion of Science (MY) and Kobayashi Foundation for Cancer Research (MY). We thank Dr T. Sugino for his helpful discussion. We also thank Mrs H. Koike, Mrs M. Araake-MIzoguchi for their technical assistance and Mrs K. Shiina for her secretarial support.

Disclosure Statement

The authors have no conflict of interest.

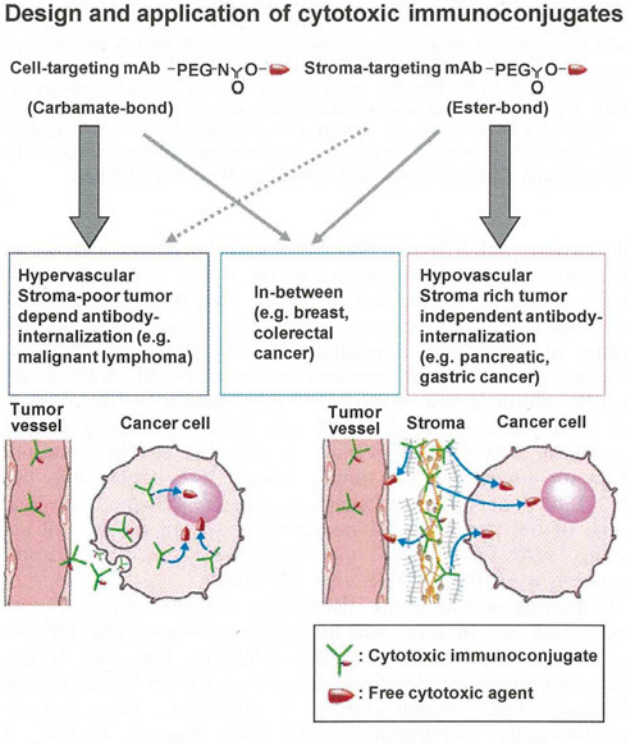

Fig. 5. Diagram of Immunoconjugate strategy to tumor tissue component and characteristic of cancer-cells. Design and application of cytotoxic immunoconjugates. SN-38 conjugated cell-targeting monoclonal antibody (mAb) via carbamate-bond is suitable for hypervascular, stroma-poor tumor dependent antibody-internalization. SN-38 conjugated stroma-targeting mAb via ester-bond is suitable for hypovascular, stroma-rich tumor independent antibody-internalization.

doi: 10.1111/cas.12062

References

1 Imai K, Takaoka A. Comparing antibody and small-molecule therapies for cancer. *Nat Rev Cancer* 2006; **6**: 714–27.
2 Matsumura Y, Maeda H. A new concept for macromolecular therapeutics in cancer chemotherapy: mechanism of tumoritropic accumulation of proteins and the antitumor agent smancs. *Cancer Res* 1986; **46**: 6387–92.
3 Duncan R. The dawning era of polymer therapeutics. *Nat Rev Drug Discov* 2003; **2**: 347–60.
4 Matsumura Y, Kataoka K. Preclinical and clinical studies of anticancer agent-incorporating polymer micelles. *Cancer Sci* 2009; **100**: 572–9.
5 Ricart AD, Tolcher AW. Technology insight: cytotoxic drug immunoconjugates for cancer therapy. *Nat Clin Pract Oncol* 2007; **4**: 245–55.
6 Doronina SO, Toki BE, Torgov MY *et al.* Development of potent monoclonal antibody auristatin conjugates for cancer therapy. *Nat Biotechnol* 2003; **21**: 778–84.
7 Wu AM, Senter PD. Arming antibodies: prospects and challenges for immunoconjugates. *Nat Biotechnol* 2005; **23**: 1137–46.
8 Doronina SO, Bovee TD, Meyer DW *et al.* Novel peptide linkers for highly potent antibody-auristatin conjugate. *Bioconjug Chem* 2008; **19**: 1960–3.
9 Koenders PG, Peters WH, Wobbes T, Beex LV, Nagengast FM, Benraad TJ. Epidermal growth factor receptor levels are lower in carcinomatous than in normal colorectal tissue. *Br J Cancer* 1992; **65**: 189–92.
10 Messersmith W, Oppenheimer D, Peralba J *et al.* Assessment of epidermal growth factor receptor (EGFR) signaling in paired colorectal cancer and normal colon tissue samples using computer-aided immunohistochemical analysis. *Cancer Biol Ther* 2005; **4**: 1381–6.
11 Hayden E. Cancer complexity slows quest for cure. *Nature* 2006; **455**: 148.
12 Heng HH, Bremer SW, Stevens JB, Ye KJ, Liu G, Ye CJ. Genetic and epigenetic heterogeneity in cancer: a genome-centric perspective. *J Cell Physiol* 2009; **220**: 538–47.
13 Collins BE, Blixt O, Han S *et al.* High-affinity ligand probes of CD22 overcome the threshold set by cis ligands to allow for binding, endocytosis, and killing of B cells. *J Immunol* 2006; **177**: 2994–3003.
14 Schmidt MM, Thurber GM, Wittrup KD. Kinetics of anti-carcinoembryonic antigen antibody-internalization: effects of affinity, bivalency, and stability. *Cancer Immunol Immunother* 2008; **57**: 1879–90.
15 Burke PJ, Senter PD, Meyer DW *et al.* Design, synthesis, and biological evaluation of antibody-drug conjugates comprised of potent camptothecin analogues. *Bioconjug Chem* 2009; **20**: 1242–50.
16 Coyne CP, Jones T, Pharr T. Synthesis of a covalent gemcitabine-(carbamate)-[anti-HER2/neu] immunochemotherapeutic and its cytotoxic anti-neoplastic activity against chemotherapeutic-resistant SKBr-3 mammary carcinoma. *Bioorg Med Chem* 2011; **19**: 67–76.
17 Dvorak HF. Tumors: wounds that do not heal. Similarities between tumor stroma generation and wound healing. *N Engl J Med* 1986; **315**: 1650–9.
18 Minchinton AI, Tannock IF. Drug penetration in solid tumors. *Nat Rev Cancer* 2006; **6**: 583–92.
19 Trédan O, Galmarini CM, Patel K, Tannock IF. Drug resistance and the solid tumor microenvironment. *J Natl Cancer Inst* 2007; **99**: 1441–54.
20 Ghajar CM, Bissell MJ. Extracellular matrix control of mammary gland morphogenesis and tumorigenesis: insights from imaging. *Histochem Cell Biol* 2008; **130**: 1105–18.
21 Yasunaga M, Manabe S, Tarin D, Matsumura Y. Cancer-stroma targeting therapy by cytotoxic immunoconjugate bound to the collagen 4 network in the tumor tissue. *Bioconjug Chem* 2011; **22**: 1776–83.
22 Yasunaga M, Manabe S, Matsumura Y. New concept of cytotoxic immunoconjugate therapy targeting cancer-induced fibrin clots. *Cancer Sci* 2011; **102**: 1396–402.
23 Ostermann E, Garin-Chesa P, Heider KH *et al.* Effective immunoconjugate therapy in cancer models targeting a serine protease of tumor fibroblasts. *Clin Cancer Res* 2008; **14**: 4584–92.
24 Palumbo A, Hauler F, Dziunycz P *et al.* A chemically modified antibody mediates complete eradication of tumors by selective disruption of tumor blood vessels. *Br J Cancer* 2011; **104**: 1106–15.
25 Armstrong A, Eck SL. EpCAM: a new therapeutic target for an old cancer antigen. *Cancer Biol Ther* 2003; **2**: 320–6.
26 Iwamura T, Katsuki T, Ide K. Establishment and characterization of a human pancreatic cancer cell line (SUIT-2) producing carcinoembryonic antigen and carbohydrate antigen 19–9. *Jpn J Cancer Res* 1987; **78**: 54–62.
27 Folli S, Westermann P, Braichotte D *et al.* Antibody-indocyanin conjugates for immunophotodetection of human squamous cell carcinoma in nude mice. *Cancer Res* 1994; **54**: 2643–9.
28 Mariani G, Lasku A, Balza E *et al.* Tumor targeting potential of the monoclonal antibody BC-1 against oncofetal fibronectin in nude mice bearing human tumor implants. *Cancer* 1997; **80**: 2378–84.
29 Senter PD, Beam KS, Mixan B, Wahl AF. Identification and activities of human carboxylesterases for the activation of CPT-11, a clinically approved anticancer drug. *Bioconjug Chem* 2001; **12**: 1074–80.
30 Li B, Sedlacek M, Manoharan I *et al.* Butyrylcholinesterase, paraoxonase, and albumin esterase, but not carboxylesterase, are present in human plasma. *Biochem Pharmacol* 2005; **70**: 1673–84.
31 Pommier Y, Topoisomerase I. inhibitors: camptothecins and beyond. *Nat Rev Cancer* 2006; **6**: 789–802.
32 Zhao H, Rubio B, Sapra P *et al.* Novel prodrugs of SN38 using multiarm poly(ethylene glycol) linkers. *Bioconjug Chem* 2008; **19**: 849–59.
33 Michel RB, Mattes MJ. Intracellular accumulation of the anti-CD20 antibody 1F5 in B-lymphoma cells. *Clin Cancer Res* 2002; **8**: 2701–13.
34 Luqman M, Klabunde S, Lin K *et al.* The antileukemia activity of a human anti-CD40 antagonist antibody, HCD122, on human chronic lymphocytic leukemia cells. *Blood* 2008; **112**: 711–20.
35 Lim SH, Vaughan AT, Ashton-Key M *et al.* Fc gamma receptor IIb on target B cells promotes rituximab internalization and reduces clinical efficacy. *Blood* 2011; **118**: 2530–40.
36 Beers SA, French RR, Chan HTC *et al.* Antigenic modulation limits the efficacy of anti-CD20 antibodies: implications for antibody selection. *Blood* 2010; **115**: 5191–201.
37 Sutherland R, Buchegger F, Schreyer M, Vacca A, Mach J-P. Penetration and binding of radiolabeled anti-carcinoembryonic antigen monoclonal antibodies and their antigen binding fragments in human colon multicellular tumor spheroids. *Cancer Res* 1987; **47**: 1627–33.
38 Hamaguchi T, Doi T, Eguchi-Nakajima T *et al.* Phase I study of NK012, a novel SN-38-incorporating micellar nanoparticle, in adult patients with solid tumors. *Clin Cancer Res* 2010; **16**: 5058–66.
39 Matsumura Y. Preclinical and clinical studies of NK012, an SN-38-incorpo -rating polymeric micelles, which is designed based on EPR effect. *Adv Drug Deliv Rev* 2011; **63**: 184–92.
40 Matsumura Y. Cancer stromal targeting (CAST) therapy. *Adv Drug Deliv Rev* 2012; **64**: 710–9.
41 Cunningham D, Humblet Y, Siena S *et al.* Cetuximab monotherapy and cetuximab plus irinotecan in irinotecan-refractory metastatic colorectal cancer. *N Engl J Med* 2004; **351**: 337–45.

Supporting Information

Additional Supporting Information may be found in the online version of this article:

Data S1. Detailed methods including linker-SN-38 derivative synthesis.

Targeted Polymeric Micelles for siRNA Treatment of Experimental Cancer by Intravenous Injection

R. James Christie,[†] Yu Matsumoto,[†,‡,§] Kanjiro Miyata,[†] Takahiro Nomoto,[⊥] Shigeto Fukushima,[∥] Kensuke Osada,[∥] Julien Halnaut,[¶] Frederico Pittella,[∥] Hyun Jin Kim,[∥] Nobuhiro Nishiyama,[†] and Kazunori Kataoka[†,⊥,∥,#,*]

[†]Division of Clinical Biotechnology, Center for Disease Biology and Integrative Medicine, Graduate School of Medicine and [‡]Department of Otorhinolaryngology and Head and Neck Surgery, Graduate School of Medicine and Faculty of Medicine, The University of Tokyo, Japan, [§]Department of Otorhinolaryngology and Head and Neck Surgery, Mitsui Memorial Hospital, Japan, and [⊥]Department of Bioengineering and [∥]Department of Materials Engineering, Graduate School of Engineering, [¶]Center for Medical System Innovation, International Student Exchange Program, and [#]Center for NanoBio Integration, The University of Tokyo, Japan

ABSTRACT Small interfering ribonucleic acid (siRNA) cancer therapies administered by intravenous injection require a delivery system for transport from the bloodstream into the cytoplasm of diseased cells to perform the function of gene silencing. Here we describe nanosized polymeric micelles that deliver siRNA to solid tumors and elicit a therapeutic effect. Stable multifunctional micelle structures on the order of 45 nm in size formed by spontaneous self-assembly of block copolymers with siRNA. Block copolymers used for micelle formation were designed and synthesized to contain three main features: a siRNA binding segment containing thiols, a hydrophilic nonbinding segment, and a cell-surface binding peptide. Specifically, poly(ethylene glycol)-*block*-poly(L-lysine) (PEG-*b*-PLL) comprising lysine amines modified with 2-iminothiolane (2IT) and the cyclo-Arg-Gly-Asp (cRGD) peptide on the PEG terminus was used. Modification of PEG-*b*-PLL with 2IT led to improved control of micelle formation and also increased stability in the blood compartment, while installation of the cRGD peptide improved biological activity. Incorporation of siRNA into stable micelle structures containing the cRGD peptide resulted in increased gene silencing ability, improved cell uptake, and broader subcellular distribution *in vitro* and also improved accumulation in both the tumor mass and tumor-associated blood vessels following intravenous injection into mice. Furthermore, stable and targeted micelles inhibited the growth of subcutaneous HeLa tumor models and demonstrated gene silencing in the tumor mass following treatment with antiangiogenic siRNAs. This new micellar nanomedicine could potentially expand the utility of siRNA-based therapies for cancer treatments that require intravenous injection.

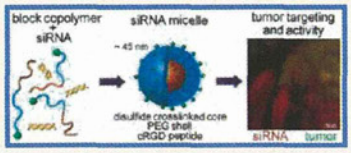

KEYWORDS: siRNA delivery · block copolymer · micelle · cRGD · cancer therapy

Small interfering ribonucleic acid (siRNA) therapeutics have great potential for treatment of disease through inhibition of protein expression, but transfer of this technology to the clinic has proven to be a great challenge. siRNA-based therapies block the expression of aberrant proteins using a natural subcellular pathway that degrades messenger RNA (mRNA) based on the nucleotide sequence contained in the siRNA molecule, a process known as RNA interference (RNAi).[1] siRNA is a 20–23 base pair degradation product generated from longer double-stranded RNA and represents the smallest double-stranded RNA deliverable that can gain access to the RNAi pathway. Potent inhibition of gene expression can be achieved due to the catalytic nature of RNAi, which results in formation of an activated RNA-induced silencing complex (RISC) that can degrade multiple strands of mRNA that are complementary to the loaded siRNA strand.[2]

The molecular machinery necessary for RNAi is located in the cell cytoplasm, thus therapeutic siRNA must also localize in the cytoplasm to exert the desired effect of protein knockdown. However, siRNA is a large water-soluble polyion (~13 000 MW) that has unique delivery obstacles not typically encountered with small hydrophobic molecules such as anticancer drugs. Due to its large size and anionic nature, siRNA cannot readily diffuse across cell membranes and requires active internalization into cells by endocytosis. Furthermore, administration of siRNA by systemic injection is challenging due to the immunogenicity of naked siRNA, degradation into inactive fragments by enzymatic activity, high renal clearance, and overall poor accumulation at target sites.[3–6] Efforts to overcome the above-mentioned obstacles has resulted in development of next-generation siRNA delivery strategies including chemically modified siRNAs that increase stability and suppress immune system activation, as well

* Address correspondence to kataoka@bmw.t.u-tokyo.ac.jp.

Received for review March 2, 2012 and accepted May 10, 2012.

Published online May 10, 2012
10.1021/nn300942b

as development of many types of particle-based systems that reversibly encapsulate siRNA. Particle-based systems are often designed to exploit the large polyanionic structure of siRNA to form polyion complexes which assemble into aggregates, vesicles, or micelles. Such particles have been prepared from cationic lipids, lipidoids, peptides, as well as synthetic polymers and block copolymers and are typically several tens to hundreds of nanometers in size. The most sophisticated delivery systems to date include features such as a PEG coating to control particle morphology and reduce nonspecific interactions with biological components, reversible cross-links for site-specific release of siRNA, environment-sensitive polymers or peptides to assist subcellular trafficking, and cell-targeting moieties to improve cell uptake and specificity. Several excellent reviews describing siRNA delivery systems in detail have recently been published.[7−14]

In this report, we introduce a nanomedicine capable of encapsulating siRNA and then delivering it through the bloodstream to tumor models in mice. This micellar siRNA delivery system was prepared using a block copolymer containing features to improve micelle stability and biological activity. Block copolymer chemistry was chosen based on our previous work with poly(ethylene glycol)-*block*-poly(L-lysine) (PEG-*b*-PLL) containing lysine amines modified with 2-iminothiolane (2IT). We found that this polymer formed nanosized micelle structures with siRNA, which prolonged blood circulation; however, RNAi activity was low.[15,16] Here, we further improved the performance of micelles by incorporating a short peptide on the micelle surface to enhance cell uptake and distribution of siRNA on the subcellular and whole organism levels. Specifically, we used the cyclo-arginine-glycine-glutamic acid (cRGD) peptide, which binds to integrin receptors that are displayed on the surface of several types of tumors and also endothelial cells associated with growing tumors.[17−20] Addition of the cRGD peptide to the micelle structure resulted in a targeted nanoparticle capable of directing siRNA to the site of activity, improving tumor accumulation and cell uptake following intravenous injection. We found that the cRGD-containing micelles improved siRNA activity both *in vitro* and *in vivo* through a combination of improved cell uptake, broadened subcellular distribution, blood stability, and tumor accumulation.

RESULTS AND DISCUSSION

Design and Synthesis of Block Copolymers. Formation of micelles with siRNA requires a material capable of binding a large polyanion and also directing assembly into higher ordered multimolecular structures. Such necessities can be fulfilled by block copolymers, which contain regions of distinctly different chemistries tailored to meet functional demands. Block copolymers used to facilitate micelle formation with siRNA in this work were designed and synthesized to contain three basic features: (i) a cationic segment with thiol groups, (ii) a hydrophilic and biologically benign segment, and (iii) a cell-surface-targeting moiety. This polymer design facilitates micelle formation following electrostatic interaction between oppositely charged macromolecules, resulting in charge neutralization and self-assembly into micelle structures with siRNA contained in the core which is surrounded by a PEG shell. Since polymers and siRNA self-assemble into core−shell micelle structures, modification of the distal end of PEG allows presentation of bioactive moieties, such as the cRGD peptide, on the micelle surface. Chemically, these features were produced from an acetal-PEG-*b*-PLL block copolymer, with the PLL segment serving as the siRNA binding region and also the point of chemical modification by reaction with lysine amines. Acetal functionality contained on the PEG terminus provided a protected aldehyde that was regenerated at low pH to provide the site of attachment for the cRGD peptide by reaction with an N-terminal cysteine residue.[21]

In our previous work, we found that PEG-*b*-PLL alone does not form stable micelle structures with siRNA, so we further modified PEG-*b*-PLL amines with 2IT to introduce amidines and free thiols into the lysine segment of the block copolymer. This modification was aimed to improve the stability of micelle structures through disulfide cross-linking in the core, which can also provide environment-sensitive stabilization of micelle structures following reduction of the covalent disulfide cross-links by free thiols in solution. Disulfide reduction is likely to occur faster within cells than in the bloodstream due to higher glutathione concentrations inside of cells, thus offering site-specific siRNA release functionality.[22] While 2IT modification of PEG-*b*-PLL resulted in the introduction of thiol groups, it also resulted in the formation of cyclic N-substituted 2-iminothiolane ring structures in the lysine side chains, which also showed a micelle-stabilizing effect.[16]

The overall synthesis scheme for preparation of modified polymers starting from acetal-PEG-*b*-PLL (PEG M_w = 12 000, PLL degree of polymerization = 45) is shown in Scheme 1. First, acetal-PEG-*b*-PLL was reacted with excess cRGD peptide at pH 4.0 to produce the peptide−polymer conjugate *via* thiazolidine ring formation between the aldehyde generated on PEG and the N-terminal cysteine residue contained on the cRGD peptide. Analysis of the peptide−polymer conjugate by ^{1}H NMR showed that the reaction was successful, with the appearance of cRGD benzyl protons (D-phenyl alanine) observed (Figure 1A). Further analysis of the integration values determined that ~80% of polymer chains contained conjugated cRGD.

Next, cRGD-PEG-*b*-PLL or acetal-PEG-*b*-PLL was reacted with 2IT to produce cRGD-PEG-*b*-PLL(2IT) and PEG-*b*-PLL(2IT), respectively. For simplicity, polymers

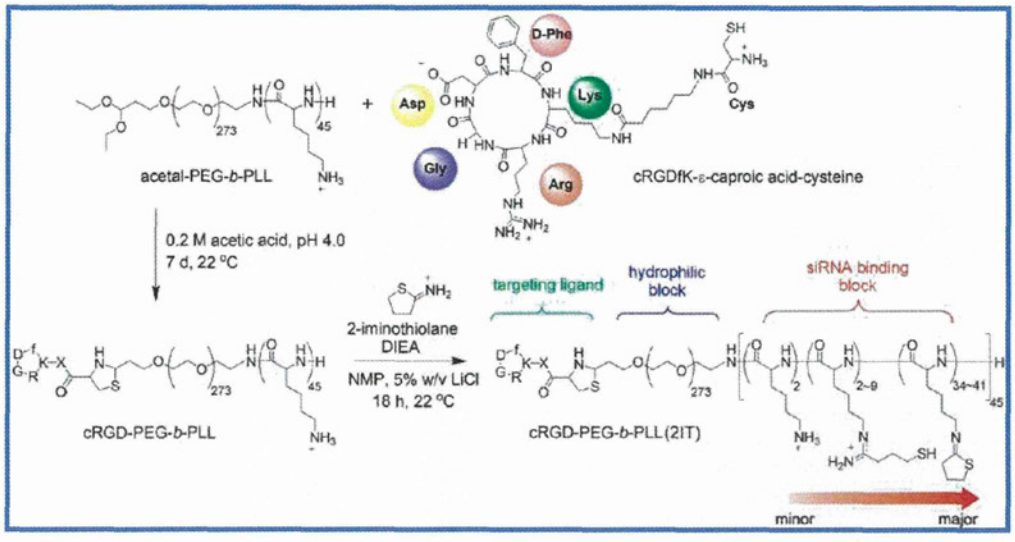

Scheme 1. Modification of PEG-*b*-PLL with cRGD and 2-iminothiolane.

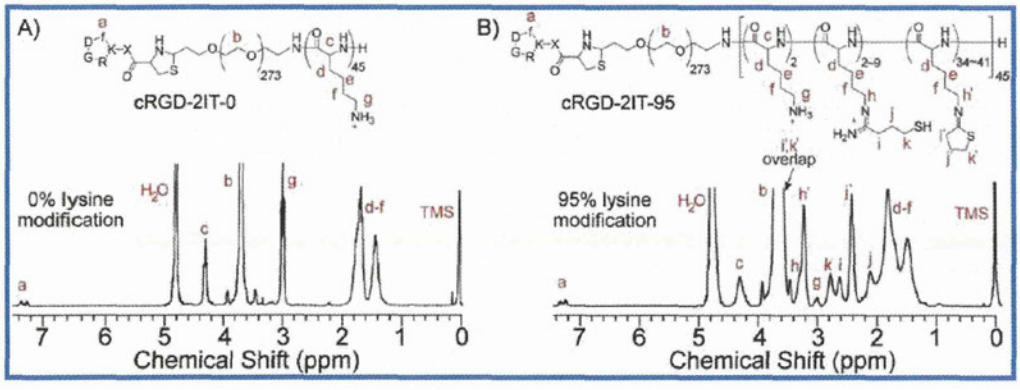

Figure 1. Characterization of polymer products. (A) ^{1}H NMR spectrum of cRGD-PEG-*b*-PLL recorded in D_2O. (B) ^{1}H NMR spectrum of cRGD-PEG-*b*-PLL(2IT) recorded in D_2O containing 3 μL/mL 35% DCl. Polymer composition was estimated based on the ^{1}H NMR spectrum and also results of Ellman's assay shown in Table 1.

are denoted as *X*2IT-*Y*, with "*X*" indicating the presence of the cRGD peptide and "*Y*" indicating the degree of 2IT modification. Polymer modification proceeded *via* nucleophilic reaction of lysine amines with 2IT in the presence of an organic base, with ~2.4 molar equiv of 2IT needed for nearly complete conversion of lysine amines. The degree of 2IT modification was determined to be 95% by ^{1}H NMR analysis, using the ratio of integration values of lysine β, γ, and δ-methylene protons ($(CH_2)_3$, δ = 1.3–1.9 ppm) to values corresponding to 2IT moieties (Figure 1B). Reaction of lysine amines with 2IT generated both 1-(4-mercaptobutyl)-amidine and cyclic iminothiolane functional groups in the PLL segment of the block copolymer, and cyclic iminothiolanes were the major product (~80%) under the reaction conditions used here. Ellman's assay for free thiols revealed a polymer thiol content much lower than the degree of lysine modification, which is consistent with iminothiolane ring formation as this functional group lacks free thiols.

TABLE 1. Summary of Polymer Compositions

polymer	MW[a]	2IT modified lysines (%)[a]	free thiol content (% side chains)[b]
2IT-0	19500	0	0.08 ± 0.04
cRGD-2IT-0	20300	0	0.5 ± 0.07
2IT-95	21800	95	4.6 ± 1.6
cRGD-2IT-95	22500	95	5.1 ± 0.7

[a] Calculated from ^{1}H NMR integration values. [b] Determined by Ellman's assay.

Preparation of Micelles. Micelle structures formed spontaneously upon mixing block copolymer with siRNA, and the theoretical configuration of the particle showing siRNA in the core, a PEG shell, and the cRGD peptide on the micelle surface is depicted in Figure 2A. Micelle formulations are named based on the polymer used for preparation (Table 2.) Micelle formation behavior was different between 2IT modified and unmodified polymers, as scattered light intensity (SLI) analysis showed that micelle structures only formed